Příloha 1

Acta Neuropathologica
Communications

RESEARCH

Open Access

Integrated genomic analysis reveals actionable targets in pediatric spinal cord low-grade gliomas

Adela Misove[1,2], Ales Vicha[1,2], Petr Broz[2,3], Katerina Vanova[1,2], David Sumerauer[1,2], Lucie Stolova[2],
Lucie Sramkova[2], Miroslav Koblizek[1,3], Josef Zamecnik[1,3], Martin Kyncl[4], Zuzana Holubova[4], Petr Liby[5],
Jakub Taborsky[5], Vladimir Benes III[5], Ivana Pernikova[6], David T. W. Jones[7,8], Martin Sill[9], Terezia Stancokova[10],
Lenka Krskova[1,3†] and Michal Zapotocky[1,2*†]

Abstract

Gliomas are the most common central nervous tumors in children and adolescents. However, spinal cord low-grade gliomas (sLGGs) are rare, with scarce information on tumor genomics and epigenomics. To define the molecular landscape of sLGGs, we integrated clinical data, histology, and multi-level genetic and epigenetic analyses on a consecutive cohort of 26 pediatric patients. Driver molecular alteration was found in 92% of patients (24/26). A novel variant of *KIAA1549:BRAF* fusion (*ex10:ex9*) was identified using RNA-seq in four cases. Importantly, only one-third of oncogenic drivers could be revealed using standard diagnostic methods, and two-thirds of pediatric patients with sLGGs required extensive molecular examination. The majority (23/24) of detected alterations were potentially druggable targets. Four patients in our cohort received targeted therapy with MEK or NTRK inhibitors. Three of those exhibited clinical improvement (two with trametinib, one with larotrectinib), and two patients achieved partial response. Methylation profiling was implemented to further refine the diagnosis and revealed intertumoral heterogeneity in sLGGs. Although 55% of tumors clustered with pilocytic astrocytoma, other rare entities were identified in this patient population. In particular, diffuse leptomeningeal glioneuronal tumors (n = 3) and high-grade astrocytoma with piloid features (n = 1) and pleomorphic xanthoastrocytoma (n = 1) were present. A proportion of tumors (14%) had no match with the current version of the classifier. Complex molecular genetic sLGGs characterization was invaluable to refine diagnosis, which has proven to be essential in such a rare tumor entity. Moreover, identifying a high proportion of drugable targets in sLGGs opened an opportunity for new treatment modalities.

Keywords: Spinal cord, Low-grade glioma, *KIAA1549:BRAF* fusion, *NTRK* fusion, Methylation profiling

†Lenka Krskova and Michal Zapotocky contributed equally to this work

*Correspondence: michal.zapotocky@fnmotol.cz

² Department of Pediatric Haematology and Oncology, Second Faculty of Medicine, Charles University and University Hospital Motol, Prague, Czech Republic
Full list of author information is available at the end of the article

Introduction

The majority of CNS tumors are located intracranially, and only 5% occur in the spinal cord [1]. Intramedullary spinal cord tumors have a glial origin and are biologically low-grade in 95%. Similarly, as in brain low-grade gliomas (LGGs), spinal cord (=intramedullary) low-grade gliomas in children (sLGGs) show a chronic course of the disease affecting the quality of life while the overall survival remains excellent [2]. Treatment of choice is maximal safe surgical resection under intraoperative

Misove *et al. Acta Neuropathologica Communications* (2022) 10:143

Page 2 of 11

monitoring which must not endanger neurological function as chemotherapy can stabilize the progression of the disease in 40–50% [3, 4].

The urge is to predict the risk of progression and search for novel, effective treatment approaches. Molecular data are seldom, suggesting that the most prevalent alteration is *KIAA1549:BRAF* fusion [5]. Due to the rarity of the disease, genomic data are scarce or incomplete, and the use of targeted therapy in sLGGs was not demonstrated yet. Therefore, an institutional integrated clinical and comprehensive genetic study was conducted to reveal sLGG-associated molecular alterations and their therapeutic implications, assess intertumoral heterogeneity using methylation profiling, and demonstrate the effect of targeted therapy in this group of patients.

Methods

Patient cohort and clinical follow-up

Tumor samples and clinical data from patients with sLGGs diagnosed and treated at our center from 2000 to 2021 were retrieved for survival, radiologic data, and molecular evaluation. Patients were followed on an outpatient or in-patient basis with regular MRI imaging. All clinical data were collected retrospectively. The last patient was enrolled on 02/11/2020, and the disease status for all patients was updated on 01/07/2021. The institutional review board approved the study, and all patients obtained informed consent as per our routine procedure.

Volumetric analysis

Volumetric analysis was implemented to measure tumor response to the targeted therapy. Lesions' volumes were estimated with open-source software 3D Slicer (version 4.10.2) using basic modules (Segment Editor, Segment Statistics) [6]. MRI sequences with the best spatial and contrast resolution were selected from available examinations for lesion volume evaluation.

DNA and RNA extraction

The nucleic acids were extracted from formalin-fixed, paraffin-embedded tissue block using QIAamp DNA FFPE Tissue Kit (Quiagen, Germany) for genomic DNA and using high pure RNA paraffin kit (Roche Diagnostics, Mannheim, Germany) for total RNA. In the case of fresh frozen sections, extraction of genomic DNA and total RNA was manufactured using Trizol Reagent (Life Technologies, Merelbeke, Belgium). Neuropathologists selected the most representative tissue blocks containing the maximum percentage of tumor tissue before isolation of nucleic acid.

cDNA synthesis and conventional RT-PCR

cDNA was prepared from RNA (Life Technologies, Carlsbad, CA) according to the manufacturer's instructions. cDNA was subjected to conventional RT-PCR amplification with primers specific for common *KIAA1549:BRAF* variants(*ex16:ex9*, *ex15:ex9*, *ex16:ex11*) as previously described [7].

Sanger sequencing

PCR and Sanger sequencing were conducted to examine hotspot mutations at codons 27 and 34 of *H3F3A*, codon 600 of *BRAF* ex15, codons 546 and 656 of *FGFR1* ex12, and codon of *FGFR1* ex14 using previously described primer pairs. Amplification was performed using $2 \times$ PCRBIO HS Taq Mix Red (PCR Biosystems Ltd., London, UK). The PCR products were electrophoresed in a 1.5% agarose gel and were recovered using the Gel DNA Fragments Extraction Kit (Geneaid, Taiwan). Sanger sequencing was performed using Big Dye Terminator v 3.1 chemistry (LifeTechnologies) and an ABI PRISM 3130 genetic analyzer Applied Biosystems. Results were analyzed using Chromaslite 2.01 (Technelysium, PtyLtd, Brisbane, Australia).

MLPA

SALSA® MLPA® probemix P370 can be used to detect genomic duplications leading to the *KIAA1549:BRAF*, *SRGAP3:RAF1*, and *FGFR1:TACC1* fusion genes and for detection of copy number aberrations in the *BRAF, CDKN2A/2B, FGFR1, MYB*, and *MYBL1* genes. Furthermore, this probemix contains five specific probes detecting the BRAF p.V600E & four predominant IDH1 p.R132H and p.R132C and IDH2 p.R172M and p.R172K point mutations, which will only generate a signal when the mutation is present. MLPA was performed following the manufacturer's instructions. Data were analyzed using Coffalyser Software (MRC-Holland, Amsterdam, The Netherlands).

RNA panel sequencing

Based on the quality of preserved nucleic acid in the samples, we were using one of Archer® FusionPlex® (Archer DX, Boulder, Colorado) commercially available panels— either Lung kit or Oncology Research kit. Despite different nucleic acid quality requirements resulting from the different number of analyzed genes, both panels are used for fusion and SNV identification with the advantage of identifying the fusion even with an unknown partner. Archer® FusionPlex® also offers robust performance even for FFPE samples. RNA extraction, library preparation, and parallel sequencing were performed as per the manufacturer's recommendation. Anchored Multiplex

Misove *et al. Acta Neuropathologica Communications* (2022) 10:143

Page 3 of 11

polymerase chain reaction amplicons were sequenced on Illumina MiSeq, and the data were analyzed using the Archer and Arriba [8] (https://github.com/suhrig/arriba/) softwares. RT-PCR was performed to validate the fusion transcript identified by RNA sequencing (Additional file 1: Table S1).

Methylation profiling
DNA methylation was performed using the Infinium Methylation EPICBeadChip Kit (Illumina, San Diego, CA, USA). A total of 250 ng of DNA from fresh frozen tumor tissue was treated with bisulfite conversion using the ZymoResearch EZ DNA Methylation kit (Zymo Research Corp, Irvine, CA, USA). In the case of FFPE samples, DNA restoration was performed as per the manufacturer's instructions (Infinium FFPE DNA Restoration kit, Illumina, San Diego, CA, USA). According to the manufacturer's explicit specifications, the Infinium HD Methylation Assay was performed at the laboratories of the Department of Pediatric Haematology and Oncology, Second Faculty of Medicine in Prague. The methylation class was established using web-based analysis via https://www.molecularneuropathology.org/ using publically available v11b4 and v12.5 versions of brain classifier. To compare spinal cord glioma samples with the DKFZ reference cohort, t-SNE analysis was performed with 10,000 most differentially methylated probes using Rtsne package v.0.13 as previously described [9].

Statistical analysis
Progression-free survival and overall survival were analyzed by the Kaplan–Meier method, and p-values reported using the log-rank test in an open-source R statistical environment (v4.1.2), using R packages survival (v2.41–3), and ggplot2 (v2.2.1).

Results
Patient selection
During the study period, 42 pediatric patients with spinal cord tumors were diagnosed, excluding non-biopsied patients with known Neurofibromatosis type 2. Diagnosis of sLGGs was made in 23 patients; 12 patients were diagnosed with ependymoma, and four patients with ATRT or other entity (Fig. 1a). Retrospective evaluation of the spinal cord tumor cohort revealed discordance between histology and the clinical course of the disease in three patients. Additional testing done in 2 ependymoma patients with atypical clinical course revealed rather glial tumors with ependymal features. Furthermore, one long-term surviving patient with an inoperable tumor initially described as anaplastic astrocytoma showed rather low-grade biology of the tumor with multiple progressions over many years of follow-up. In this particular patient, molecular studies revealed *NTRK2* fusion and confirmed a glial origin of the tumors with low-grade behavior. Therefore, these three patients were added to the sLGGs group in this article to a total number of 26 patients (Additional file 2: Table S2; sLGG_01—sLGG_26), representing 7% of all institutional pediatric LGGs (total number = 350). Median age at diagnosis for the sLGGs group was 4.55 years (range from 1.15 to 17.54 years). Histologically, the sLGGs group comprised predominantly of pilocytic astrocytoma, diffuse astrocytoma, and ganglioglioma.

Comprehensive genomic analysis uncovered a novel and rare alterations within the MAPK pathway
Comprehensive genetic analysis consisting of Sanger sequencing, MLPA, and RNA sequencing was employed to determine the genetic landscape of pediatric LGGs. Oncogenic driver alterations were detected in 93% (n = 24) of patients; no alterations were detected in two patients where analysis failed due to insufficient tissue quality. Alterations found across sLGGs could be classified into two groups (Fig. 1b: 1) *BRAF* alteration consisting of *KIAA1549:BRAF* fusions (75%) with the high occurrence of rare and novel fusion variants, and non-KIAA1549:*BRAF* fusions (8%), 2) non-*BRAF* alterations (17%). Surprisingly, no case harboring BRAFV600E or *H3F3A/HIST1H3B* mutation was identified. We also evaluated the presence of the secondary alterations and found two cases of *CDKN2A* homozygous deletion in non-*BRAF* tumors. (Fig. 1c) Furthermore, pathogenic *MET* and *EGFR* variants were detected in two *KIAA1549:BRAF* cases.

A novel variant of *KIAA1549:BRAF* fusion (*ex10:ex9*) was identified using RNA sequencing in four cases (Fig. 2a). Rare types of *KIAA1549:BRAF* fusions (*ex13:ex9, ex13:ex11, ex16:ex11, ex15:ex11*) were identified in further 21% sLGG patients. Non-canonical

(See figure on next page.)

Fig. 1 **a** Overview of the total number of 42 spinal cord tumors diagnosed within 2000–2021. **b** Pie of pie demonstrates three molecular alteration groups in sLGGs; tumors driven with canonical *BRAF* fusions, non-canonical *BRAF* fusions, and non-*BRAF* alterations. **c** Oncoplot summarizes the relation of demographic (sex, age), clinical (progression, survival), and molecular-pathology data (histology, driver alteration, *CDKN2A* status), **d** Comparison of the molecular alterations, anatomical location, and extent of the tumors. The position of vertical lines shows the anatomical location of the tumor and the length of vertical lines outlines the levels of the spinal cord affected by each tumor sample. Molecular subtypes are shown in colors. On the left side are displayed common *KIAA1549:BRAF* fusions (pink) in contrast with the right side where are rare *KIAA1549:BRAF* fusions (yellow), a novel type of *KIAA1549:BRAF* fusion (red), non-*KIAA1549:BRAF* fusions (green) and non-*BRAF* alterations (blue)
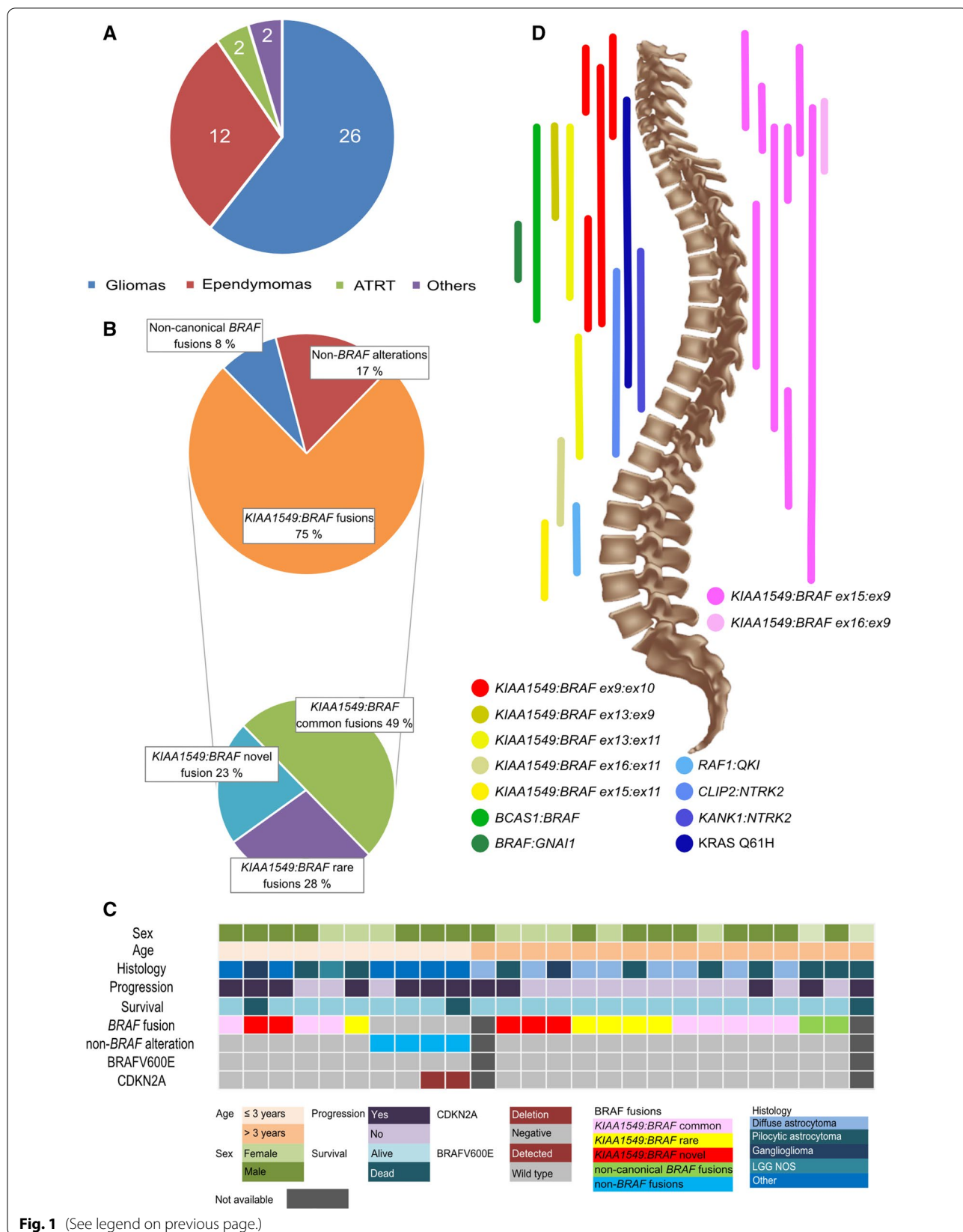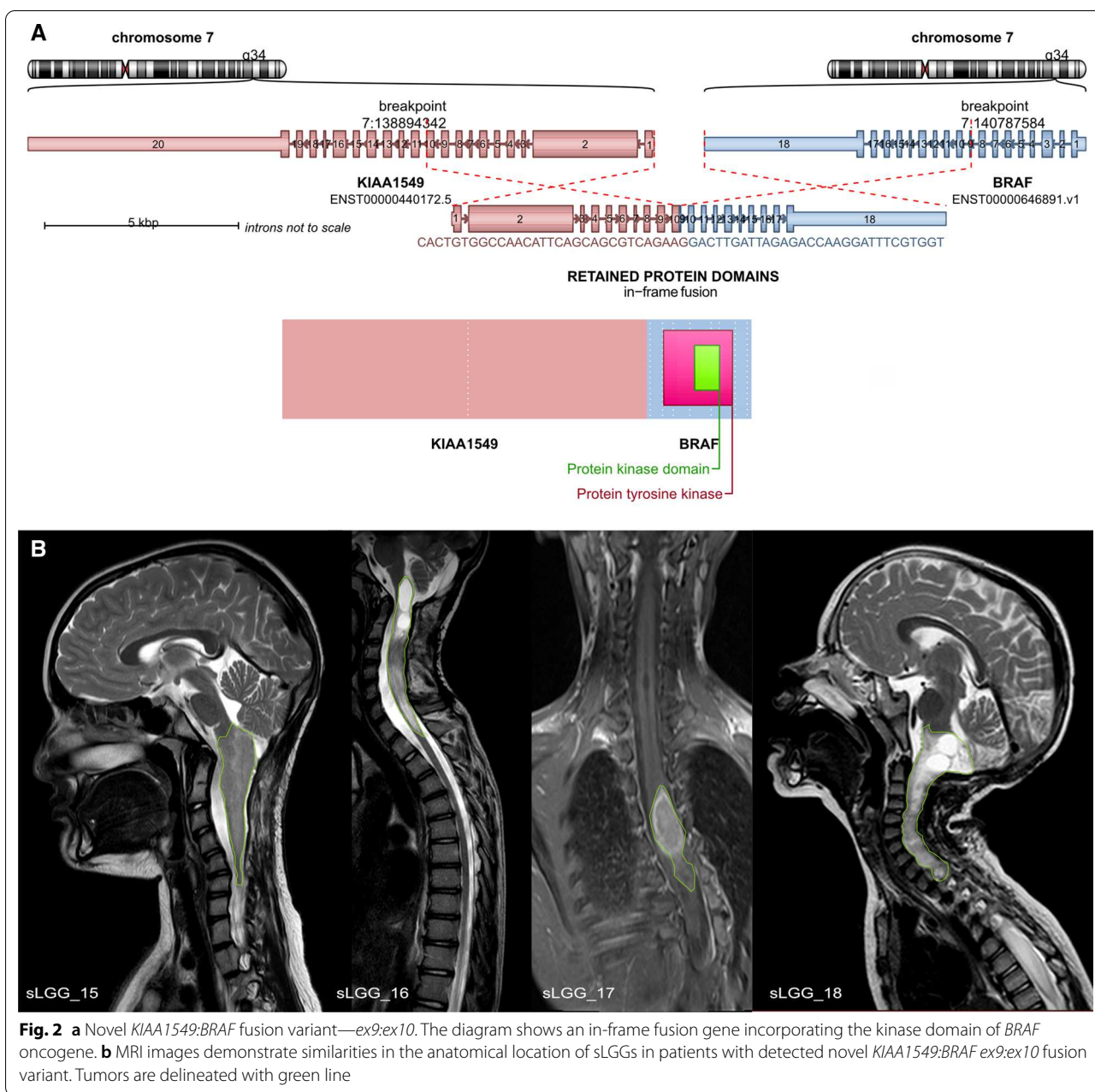
Misove *et al. Acta Neuropathologica Communications* (2022) 10:143

Page 4 of 11

Fig. 1 (See legend on previous page.)

Misove *et al. Acta Neuropathologica Communications* (2022) 10:143

Page 5 of 11

Fig. 2 **a** Novel *KIAA1549:BRAF* fusion variant—*ex9:ex10*. The diagram shows an in-frame fusion gene incorporating the kinase domain of *BRAF* oncogene. **b** MRI images demonstrate similarities in the anatomical location of sLGGs in patients with detected novel *KIAA1549:BRAF ex9:ex10* fusion variant. Tumors are delineated with green line

BRAF fusions were detected in two patients; accounting for *BCAS1:BRAF* and *GNAI1:BRAF*. Two independent methods verified those rare and novel *BRAF* fusions using RT-PCR with specific primers and chromosome 7q34 duplication using MLPA.

Anatomical distribution of the genetic alterations (Fig. 1d) interestingly showed *KIAA1549:BRAF ex10:ex9*-positive tumors located in the upper half of the spinal cord with partial medulla oblongata involvement in two cases (two cases in the cervical spine (C1–C7), one case in the cervical and upper thoracic spine (C2–T2), and

one in the upper thoracic spine (T2–T7) (Fig. 2b). To evaluate the frequency of the *KIAA1549:BRAF ex10:ex9* fusion variant, the cohort was expanded using 205 institutional cases of intracranial pediatric LGGs of various locations with known molecular drivers (Additional file 3: Fig. S1). Among more than 50 cases with detectable *KIAA1549:BRAF,* no case harbored an *ex10:ex9* variant suggesting exclusive occurrence in the spinal cord.

Non-*BRAF* alterations were detected in four tumor samples consisting of *CLIP2:NTRK2, KANK1:NTRK2, RAF1:QKI,* and KRAS Q61H. The young age of three

Misove et al. Acta Neuropathologica Communications   (2022) 10:143

Page 6 of 11

years and under at diagnosis characterized this group of patients. This group's histological appearance was not typical for LGG, and molecular testing helped refine the diagnosis. *CLIP2:NTRK2* case was diagnosed as an anaplastic astrocytoma grade 3. Despite HGG histology, the presence of *CDKN2A* homozygous deletion, and multiple progressions, the patient was alive 15 years from the time of diagnosis. Pathologists reported two cases (*KANK1:NTRK2* and *RAF1:QKI*) as ependymomas, but these tumors were reclassified as low-grade glioma due to the clinical course, underlying molecular alteration, and methylation profile. Based on the molecular profile, the case with *KANK1:NTRK2* that also harbored *CDKN2A* homozygous deletion was treated with a radiation-sparing approach using chemotherapy only as first-line therapy. Patient with sLGG harboring *RAF1:QKI* underwent subtotal resection followed by careful observation. KRAS Q61H mutated case had histology of low-grade glioneuronal tumor (LGNT), and the patient was observed only after partial resection.

Methylation profiling revealed significant intertumoral heterogeneity among sLGGs

The current version (v12.5) of the Heidelberg methylation classifier does not provide any methylation class specific for spinal cord gliomas in contrast to spinal cord ependymomas. Therefore, we performed methylation profiling to evaluate how would sLGGs be classified based on the epigenetic features and to discern intertumoral heterogeneity. The analysis was performed using publically available Heidelberg classifier v12.5. Out of 22 patients (91.6%) with sufficient tissue available, 12 tumors (55%) were predicted as pilocytic astrocytoma, subclass posterior fossa (PA-PF) despite variable calibrated scores (calibrated scores (CS) 0.35–0.99). Three tumors (14%) with 1p deletion matched with diffuse leptomeningeal glioneuronal tumor (DLGNT), methylation class 1 (DLGNT – MC1) (two CS 0.99, one CS 0.25). One anaplastic astrocytoma with *CLIP2:NTRK2* fusion was classified as anaplastic pilocytic astrocytoma (CS 0.62), currently also known as high-grade astrocytoma with piloid features (HGAP). The other *NTRK2* fused glioma (*KANK1:NTRK2*), originally diagnosed as ependymoma, was classified as pleomorphic xanthoastrocytoma (PXA) (CS 0.90). One case (*QKI:RAF1*) was clustered with a subtype A of glioneuronal tumors (CS 0.99). One case (*KIAA1549:BRAF ex10:ex9*) was classified as desmoplastic infantile ganglioglioma / desmoplastic infantile astrocytoma (CS 0.59). The remaining three tumors (14%) matched with control tissue most probably due to low tumor tissue content. Moreover, t-SNE analysis using a previously published reference cohort was performed to

further refine the methylation class prediction. As classified by v12.5, significant proportion of the samples clustered nearby PA-PF cluster. They seemed to be forming a separate cluster suggesting a possible distinction from posterior fossa pilocytic astrocytoma. Remaining samples clustered with DLGNT, GNT, PXA, and other clusters as predicted with the classifier (Fig. 3).
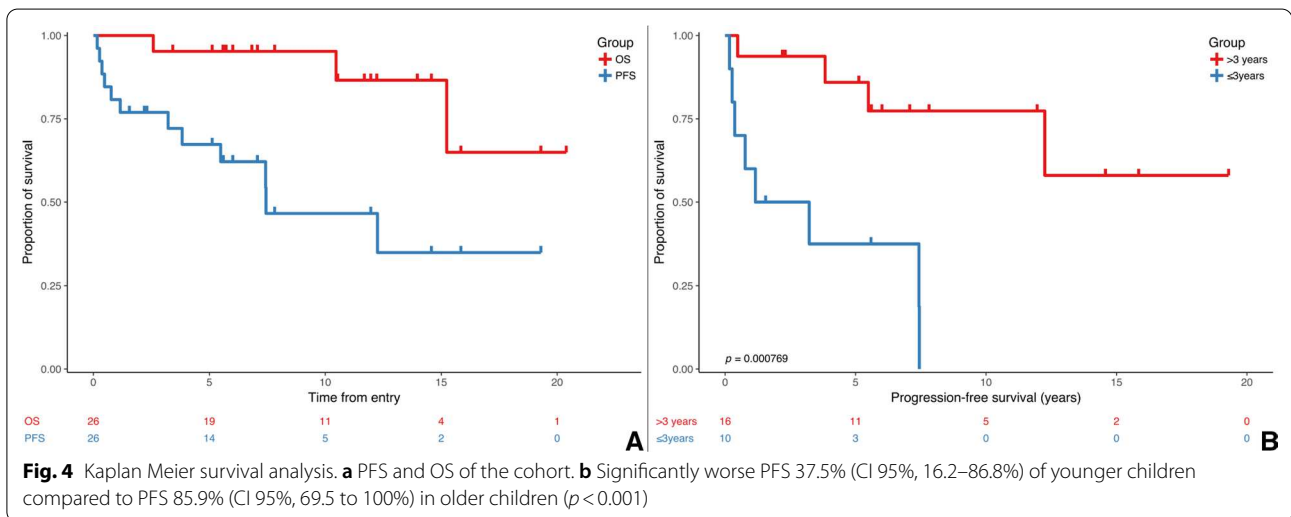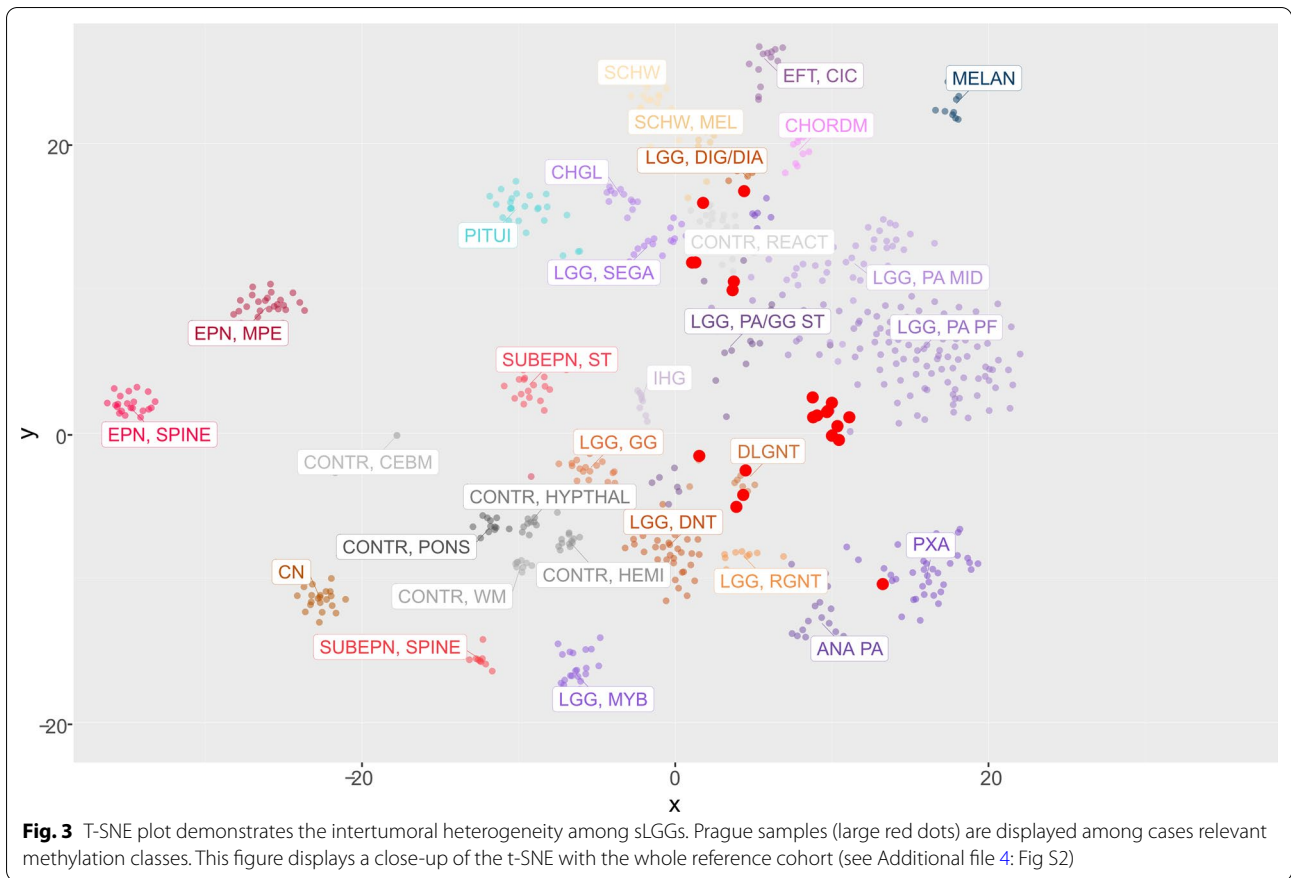
Clinical outcome and exploitation of molecular targets

At a median follow-up of 6.96 years (IQR: 3.42–12.22), 5-year progression-free survival was 67.3% (95% confidence interval [CI], 50.8–89.1%). Overall survival rate at 5 years was 95.2% (95% [CI], 86.6–100.0%) (Fig. 4a). Infants of three years and younger fared significantly worse compared to those older than three with 5-year PFS 37.5% (CI 95%, 16.2–86.8%) and 85.9% (CI 95%, 69.5–100%), respectively ($p < 0.001$) (Fig. 4b) Three patients died of the disease 15, 10, and two years after diagnosis respectively due to the progressive disease, regardless of the histological grade or molecular alteration (one with *CLIP2:NTRK2*, one without known driver alteration, and one with *KIAA1549:BRAF ex10:ex9* variant).

Based on molecularly identified targets, four patients received targeted therapy using MAPK pathway inhibitors. Three patients with *KIAA1549:BRAF* fusion were treated with MEK-inhibitor trametinib. According to the volumetric measurements, one of the patients (sLGG_15) responded with stable disease, and two patients (sLGG_06 and sLGG_07) exhibited partial responses (reduction of 51% and 61%) that were achieved after 5 and 8 months, respectively. Patient (sLGG_22) with *CLIP2:NTRK2* fusion was treated with TRK inhibitor larotrectinib with quickly induced volume reduction, not meeting partial response (40%), detectable on magnetic resonance 54 days after the therapy initiation (Fig. 5). The radiological volume reduction was accompanied by significant clinical improvement with no remarkable drug-related toxicity. Unfortunately, tumor progression accompanied by clinical decline was detected after 22 months of targeted therapy. After another five months, the patient died due to the tumor progression to the brainstem. DNA sequencing from autopsy material did not reveal any point mutations in the *NTRK1/2/3* kinase domain; thus, the mechanism of acquired resistance remained unknown [10].

Discussion
Here we present a study with comprehensive genomic and epigenomic analysis in a 20-year retrospective single institutional non-selected cohort of 26 consecutive sLGG patients in the context of clinical course,

Misove *et al. Acta Neuropathologica Communications* (2022) 10:143

Page 7 of 11

Fig. 3 T-SNE plot demonstrates the intertumoral heterogeneity among sLGGs. Prague samples (large red dots) are displayed among cases relevant methylation classes. This figure displays a close-up of the t-SNE with the whole reference cohort (see Additional file 4: Fig S2)

Fig. 4 Kaplan Meier survival analysis. **a** PFS and OS of the cohort. **b** Significantly worse PFS 37.5% (CI 95%, 16.2–86.8%) of younger children compared to PFS 85.9% (CI 95%, 69.5 to 100%) in older children ($p < 0.001$)

including quantitative imaging analysis and employment of novel treatment modalities. New findings regarding significant epigenetic heterogeneity were for the first time reported in pediatric sLGG population. Furthermore, identification of fusion landscape including novel fusion variants highlighted the impact of our data on diagnostics and new therapeutic opportunities.

We confirmed that the majority of pediatric sLGGs harbored *KIAA1549:BRAF* fusions, but unlike intracranial
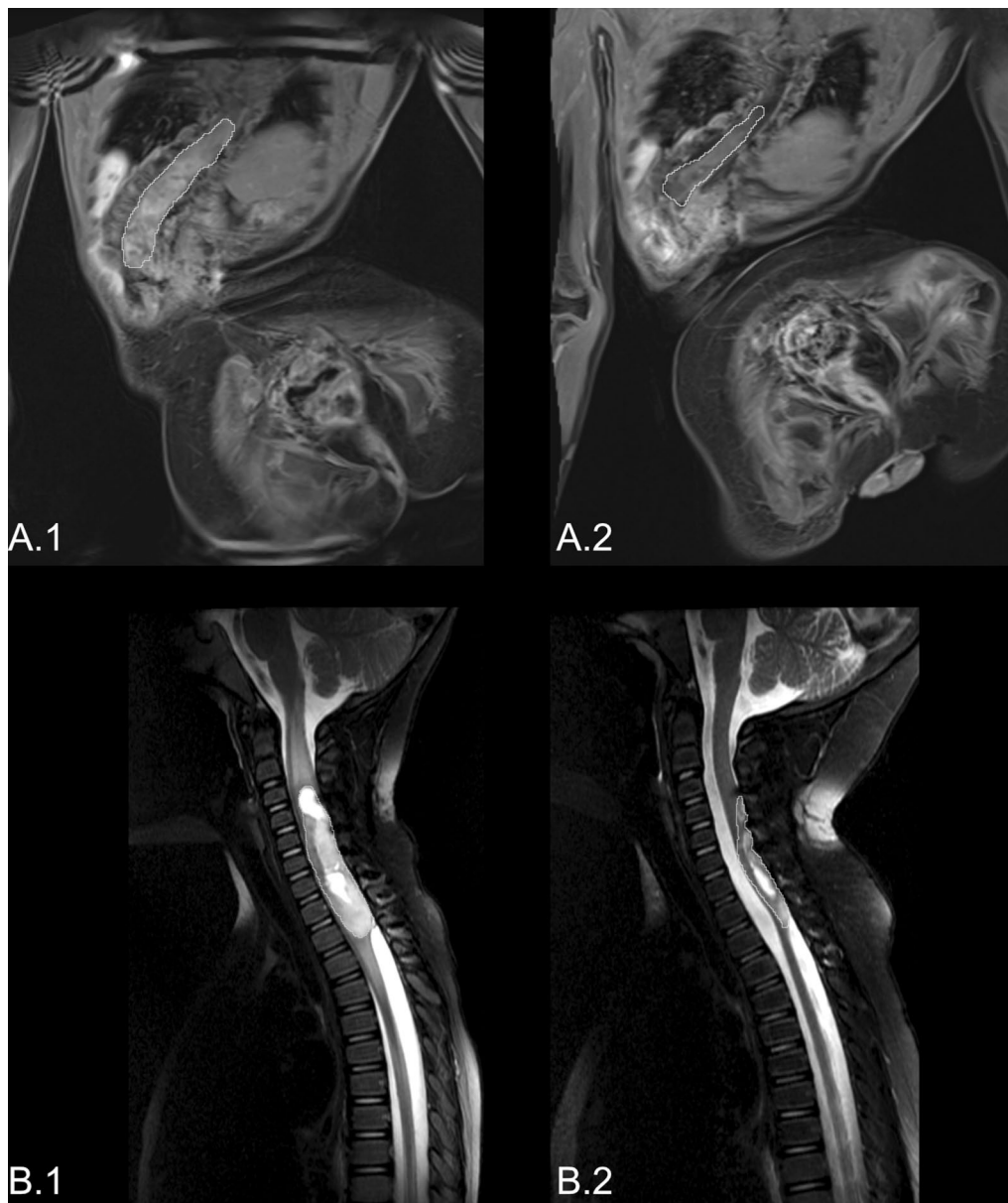
Misove *et al. Acta Neuropathologica Communications* (2022) 10:143

Page 8 of 11

Fig. 5 Radiological response to the targeted therapies. The white line (**a.1**) indicates tumor volume before initiation of NTRK inhibitor in patients sLGG_22, and (**a.2**) shows a 40% tumor volume reduction after 54 days of therapy. Likewise, the white line (**b.1**) shows tumor volume before initiation of MEK inhibitor in patient sLGG_07, and (**b.2**) shows a 61% tumor volume reduction after eight months of therapy

location, rare and novel variants were predominantly present. In particular, the novel *KIAA1549:BRAF ex10:ex9* was uncovered in our study. Importantly, this fusion variant was not found in any of our institutional pediatric intracranial LGGs cases, making this variant specific for the spinal cord compartment. Moreover, to our knowledge, this fusion variant has not been reported yet in the literature. As reported in other *KIAA1549:BRAF*

variants, the variant *ex10:ex9* also lacked the autoinhibitory domain and caused MAPK activation in the same manner [11, 12] (Fig. 2a).

Non-*BRAF* fusions were detected in children younger than three years and consisted of tumors with *NTRK2* and *RAF1* fusions and *KRAS* mutation. The clinical course of the disease in non-*BRAF* fusion patients tended to progress requiring multiple treatment

Misove *et al. Acta Neuropathologica Communications* (2022) 10:143

Page 9 of 11

modalities. Furthermore, two patients with non-canonical *BRAF* fusions (*BCAS1:BRAF, GNAI1:BRAF*) were revealed and confirmed that non-canonical *BRAF* fusions could occur in the sLGGs. Interestingly, there was no spinal cord glioblastoma characterized by histone *H3F3A* mutation in the presented cohort of spinal cord tumors [13]. No BRAF V600E mutation was detected in our cohort, probably due to a limited number of patients and a low prevalence of BRAF V600E mutation in sLGG [5, 14].

Survival in regards to 5-year PFS (67.3%) and OS (95.2%) was comparable with more extensive series with predominantly intracranial pediatric LGGs or sLGGs [5, 14]. Importantly, significantly worse PFS in younger children compared to the older ones stood out in the presented cohort. The extent of resection did not influence our PFS data as only two patients had their sLGGs completely removed. Therefore, the poorer outcome of younger children might have been related to the presence of non-*BRAF* alterations in combination with more frequent occurrence of cases with atypical histology. Our observation of a poorer prognosis was consistent with previously published clinical trials where young children fared significantly worse [15, 16]. Frequent non-*BRAF* fusions in younger children with sLGGs and histology not typical for true pediatric LGGs resembled cases of infant hemispheric gliomas, [17, 18] underlying the necessity of multi-layer diagnosis integrating histopathology and molecular genetics analysis. Some of our very young children with sLGGs were diagnosed with "ependymoma-like" histology, and further molecular investigation helped to refine the diagnosis.

Previously published studies evaluated the genomic landscape of spinal cord gliomas. More extensive series usually presented limited information on molecular alterations restricted to data from molecular biology methods such as FISH, NanoString platform, or RT-PCR [5], most probably due to poor tumor tissue availability. Grob et al. showed that 42% of sLGGs tested positive for *KIAA1549:BRAF* fusion [5]. It is essential to underline that the most frequent alterations in our cohort were rare and novel *KIAA1549:BRAF* fusion variants. The mechanism of *BRAF* activation remains the same, but commonly used diagnostic methods (RT-PCR with specific primers/NanoString) will not detect rare fusion variants, potentially compromising an opportunity for targeted therapy for those patients. The rare *KIAA1549:BRAF ex13:ex11* fusion variant was only described in one case of spinal glioneuronal tumor [19]. *RAF:QKI1* is known to activate MAPK/ERK and PI3K/mTOR signaling and was already described in a single case report of an adult diagnosed with spinal pleomorphic xanthoastrocytoma [20]. Moreover, some other larger studies focused on single

nucleotide variants rather than gene fusions in the adult population and therefore were unable to capture the whole landscape of fusions related to pediatric sLGG [21, 22].

Methylation profiling using Heidelberg classification [9] was demonstrated as a powerful research tool in pediatric CNS tumors. We employed the whole-genome DNA methylation array to uncover epigenetic features of sLGGs. A dominant cluster with the methylation class "pilocytic astrocytoma, posterior fossa" suggested a possibility of a common cell of origin with the most frequent intracranial group of LGGs. Nevertheless, the current classifier scored 55% of tumors in our sLGGs group between 0.3 and 0.97. This was in keeping with t-SNE analysis demonstrating these tumors form a cluster nearby the PA-PF cluster. This data could suggest distinct epigenetic features of sLGGs compared to PA-PF. Moreover, tumors clustering with rare methylation classes were detected, in particular DLGNT, HGAP, and PXA. Three DLGNT cases were circumscribed as spinal cord lesions without any evidence of dissemination through the neuroaxis. HGAP and PXA were represented by cases with uncharacteristic histology (not clear LGGs), either anaplastic astrocytoma or anaplastic ependymoma, presence of *NTRK2* fusions, and long-term survival. Several cases (n = 3) did not match any methylation classes suggesting either high normal tissue content or a rare entity yet to be defined [23]. Previous study attempted to characterize spinal cord gliomas using methylation profiling. The cohort consisted of 19 adults and seven children with high-grade and low-grade gliomas, and therefore a portion of cases clustered with Diffuse Midline Glioma *H3FA3*-positive and glioblastoma *IDH* wild-type. They also described two adult cases with HGAP and very short survival, two cases with IDH mutant glioma, and one DLGNT. Eight cases matched with pilocytic astrocytoma, but the tissue was not available to perform RNA sequencing, and therefore authors were not able to demonstrate the presence of characteristic fusions [24].

Comprehensive genomic analysis was critical not only to uncover the molecular landscape of pediatric sLGGs but also to identify high-priority targets for novel therapies. In particular, targeted therapy was used in four sLGGs patients with progressive disease who presented with neurological decline. Previously, MEK-inhibitor trametinib was shown to benefit a proportion of patients with progressive NF1 or *BRAF*-driven LGGs [25, 26], and our series of cases suggest clinical benefit with objective responses documented on magnetic resonance imaging in sLGGs. In addition, NTRK inhibitors have shown high efficacy in multiple NTRK-driven cancers [27], and our case demonstrated significant clinical benefit of such therapy in the patient with *NTRK2* fused sLGG.

Misove *et al. Acta Neuropathologica Communications* (2022) 10:143

Page 10 of 11

A relatively small cohort size, short follow-up, and retrospective data collection did not allow a more comprehensive prognostic marker evaluation. Furthermore, volumetry was used as a method for response evaluation considering bidimensional measurement less feasible [28], especially in our sLGG patients frequently suffering from significant spinal deformities. Therefore, response assessment in Pediatric Neuro-Oncology (RAPNO) was not implemented in this study [29].

Nevertheless, we have assembled a coherent group of solely pediatric patients with extensive molecular analysis, and our data demonstrated the importance of integrative molecular-pathological diagnosis and enlightening the potential of targeted treatment for sLGGs. Future large prospective studies evaluating prognostic markers, the efficacy of targeted therapies, and volumetric response assessment in sLGG are needed.

Conclusion

This study provides essential data on the molecular background of purely pediatric cohort of anatomically defined low-grade gliomas confined to the spinal cord. Methylation profiling revealed epigenetic landscape of sLGG demonstrating that 55% of cases cluster with posterior fossa pilocytic astrocytoma samples with the remaining 45% being very heterogeneous. Despite this epigenetic heterogeneity, sLGGs harbor driver alterations within MAPK pathway. In contrast to the intracranial LGGs, non-*BRAF* fusions (including *NTRK* fusions) and rare *KIAA1549:BRAF* variants, including novel variant *ex9:ex10*, represent frequent molecular drivers in sLGG. Our data clearly demonstrated the presence of druggable targets, and our case series demonstrated promising results in disease control with targeted therapy. However, further research and prospective clinical trials are required to evaluate the role of targeted therapy in sLGG patients.

Abbreviations

ATRT: Atypical teratoid rhabdoid tumor; cDNA: Complementary DNA; CI: Confidence interval; CS: Calibrated score; DLGNT: Diffuse leptomeningeal glioneuronal tumor; DNA: Deoxyribonucleic acid; Ex: Exon; FGFR: Fibroblast growth factor receptors; GNT: Glioneuronal tumor; HGAP: High-grade astrocytoma with piloid features; IDH: Isocitrate dehydrogenase; IQR: Interquartile range; LGG: Low-grade glioma; LGNT: Low-grade glioneuronal tumor; MAPK: Mitogen-activated protein kinase; MC: Methylation class; MEK: Mitogen-activated protein kinase kinase; MLPA: Multiplex ligation-dependent probe amplification; MRI: Magnetic resonance imaging; NTRK: Neurotrophic tyrosine receptor kinase; PA-PF: Pilocytic astrocytoma–posterior fossa; PCR: Polymerase chain reaction; PXA: Pilomyxoid astrocytoma; RAPNO: Response assessment in Pediatric Neuro-Oncology; RNA: Ribonucleic acid; RT-PCR: Reverse transcription polymerase chain reaction; sLGGs: Spinal low-grade gliomas.

Supplementary Information

The online version contains supplementary material available at https://doi.org/10.1186/s40478-022-01446-0.

Additional file 1: Table S1. Table of primers used to validate the fusion transcripts identified by RNA sequencing.

Additional file 2: Table S2. Table showing the complete sLGGs cohort emphasizing the original histology before molecular pathology reevaluation, anatomical location, and molecular-biology data.

Additional file 3: Fig. S1. A total number of pediatric intracranial LGG patients with known genetic alteration is dividedby anatomical location. Importantly, *KIAA1549:BRAF ex9:ex10* variant fusion was detected solely in the upperspine.

Additional file 4: Fig. S2. T-SNE analysis displaying Prague samples (large red dots) among reference cohort samples.

Declarations

Ethics approval and consent to participate
Ethics approval and consent were waived.

Consent for publication
Consent for publication was obtained from parent or legal guardian. Institutional consent form was used.

Competing interests
The authors declare that they have no competing interests.

Author details
[1]Prague Brain Tumor Research Group, Second Faculty of Medicine, Charles University and University Hospital Motol, Prague, Czech Republic. [2]Department of Pediatric Haematology and Oncology, Second Faculty of Medicine, Charles University and University Hospital Motol, Prague, Czech Republic. [3]Department of Pathology and Molecular Medicine, Second Faculty of Medicine, Charles University Prague and Faculty Hospital Motol, Prague, Czech Republic. [4]Department of Radiology, Second Faculty of Medicine, Charles University in Prague and Motol University Hospital, Prague, Czech Republic. [5]Department of Neurosurgery, Second Faculty of Medicine, Charles University

Misove *et al. Acta Neuropathologica Communications* (2022) 10:143

Page 11 of 11

and University Hospital Motol, Prague, Czech Republic. [6]Department of Neurology, Second Faculty of Medicine, Charles University and University Hospital Motol, Prague, Czech Republic. [7]Hopp Children's Cancer Center Heidelberg (KiTZ), Heidelberg, Germany. [8]Pediatric Glioma Research Group, German Cancer Research Center (DKFZ), Heidelberg, Germany. [9]Division of Biostatistics, German Cancer Research Center (DKFZ), Heidelberg, Germany. [10]Department of Pediatric Oncology and Hematology, Children's University Hospital, Banska Bystrica, Slovakia.

References

1. Barker DJP, Weller RO, Garfield JS (1976) Epidemiology of primary tumours of the brain and spinal cord: a regional survey in southern England. J Neurol Neurosurg Psychiatry 39:290–296
2. Constantini S, Miller DC, Allen JC, Rorke LB, Freed D, Epstein FJ (2000) Radical excision of intramedullary spinal cord tumors: surgical morbidity and long-term follow-up evaluation in 164 children and young adults. J Neurosurg Spine 93:183–193
3. Gnekow AK, Kandels D, Van TC, Azizi AA, Opocher E, Stokland T et al (2019) SIOP-E-BTG and GPOH guidelines for diagnosis and treatment of children and adolescents with low grade glioma. Klin Padiatr 231:107–135
4. Beneš V, Barsa P, Beneš V, Suchomel P (2009) Prognostic factors in intramedullary astrocytomas: a literature review. Eur Spine J 18:1397–1422
5. Grob ST, Nobre L, Campbell KR, Davies KD, Ryall S, Aisner DL et al (2020) Clinical and molecular characterization of a multi-institutional cohort of pediatric spinal cord low-grade gliomas. Neuro-Oncol Adv 2:1–9
6. Fedorov A, Beichel R, Kalpathy-Cramer J, Finet J, Fillion-Robin JC, Pujol S et al (2012) 3D Slicer as an image computing platform for the Quantitative Imaging Network. Magn Reson Imaging 30:1323–1341
7. Tian Y, Rich BE, Vena N, Craig JM, MacConaill LE, Rajaram V et al (2011) Detection of KIAA1549-BRAF fusion transcripts in formalin-fixed paraffin-embedded pediatric low-grade gliomas. J Mol Diagn 13:669–677
8. Uhrig S, Ellermann J, Walther T, Burkhardt P, Frohlich M, Hutter B et al (2021) Accurate and efficient detection of gene fusions from RNA sequencing data. Genome Res 31:448–460
9. Capper D, Jones DTW, Sill M, Hovestadt V, Schrimpf D, Sturm D et al (2018) DNA methylation-based classification of central nervous system tumours. Nature 555:469–474
10. Cocco E, Schram AM, Kulick A, Misale S, Won HH, Yaeger R et al (2019) Resistance to TRK inhibition mediated by convergent MAPK pathway activation. Nat Med 25:1422–1427
11. Jones DTW, Kocialkowski S, Liu L, Pearson DM, Bäcklund LM, Ichimura K et al (2008) Tandem duplication producing a novel oncogenic BRAF fusion gene defines the majority of pilocytic astrocytomas. Cancer Res 68:8673–8677
12. Pfister S, Janzarik W, Remke M, Ernst A, Werft W, Becker N et al (2008) BRAF gene duplication constitutes a mechanism of MAPK pathway activation in low-grade astrocytomas. J Clin Invest 118(5):1739–1749
13. Konar SK, Bir SC, Maiti TK, Nanda A (2017) A systematic review of overall survival in pediatric primary glioblastoma multiforme of the spinal cord. J Neurosurg Pediatr 19:239–248
14. Ryall S, Zapotocky M, Fukuoka K, Nobre L, Guerreiro Stucklin A, Bennett J et al (2020) Integrated molecular and clinical analysis of 1000 pediatric low-grade gliomas. Cancer Cell 37:569–583.e5
15. Ater JL, Zhou T, Holmes E, Mazewski CM, Booth TN, Freyer DR et al (2012) Randomized study of two chemotherapy regimens for treatment of low-grade glioma in young children: a report from the Children's Oncology Group. J Clin Oncol 30:2641–2647
16. Gnekow AK, Walker DA, Kandels D, Picton S, Perilongo G, Grill J et al (2017) A European randomised controlled trial of the addition of etoposide to standard vincristine and carboplatin induction as part of an 18-month treatment programme for childhood (≤16 years) low grade glioma: a final report. Eur J Cancer 81:206–225
17. Clarke M, Mackay A, Ismer B, Pickles JC, Tatevossian RG, Newman S et al (2020) Infant high-grade gliomas comprise multiple subgroups characterized by novel targetable gene fusions and favorable outcomes. Cancer Discov 10:942–963
18. Guerreiro Stucklin AS, Ryall S, Fukuoka K, Zapotocky M, Lassaletta A, Li C et al (2019) Alterations in ALK/ROS1/NTRK/MET drive a group of infantile hemispheric gliomas. Nat Commun 10:1–13
19. Chiang JCH, Harreld JH, Orr BA, Sharma S, Ismail A, Segura AD et al (2017) Low-grade spinal glioneuronal tumors with BRAF gene fusion and 1p deletion but without leptomeningeal dissemination. Acta Neuropathol 134:159–162
20. Daoud EV, Wachsmann M, Richardson TE, Mella D, Pan E, Schwarzbach A et al (2019) Spinal pleomorphic xanthoastrocytoma with a QKI-RAF1 fusion. J Neuropathol Exp Neurol 78:10–14
21. Chai RC, Zhang YW, Liu YQ, Chang YZ, Pang B, Jiang T et al (2020) The molecular characteristics of spinal cord gliomas with or without H3 K27M mutation. Acta Neuropathol Commun 8:1–11
22. Zhang M, Iyer RR, Azad TD, Wang Q, Garzon-Muvdi T, Wang J et al (2019) Genomic landscape of intramedullary spinal cord gliomas. Sci Rep 9:1–8
23. Lebrun L, Bizet M, Melendez B, Alexiou B, Absil L, Van Campenhout C et al (2021) Analyses of DNA methylation profiling in the diagnosis of intramedullary astrocytomas. J Neuropathol Exp Neurol 80:663–673
24. Biczok A, Strübing FL, Eder JM, Egensperger R, Schnell O, Zausinger S et al (2021) Molecular diagnostics helps to identify distinct subgroups of spinal astrocytomas. Acta Neuropathol Commun 9:119
25. Selt F, Van Tilburg CM, Bison B, Sievers P, Harting I, Ecker J (2020) Response to trametinib treatment in progressive pediatric low-grade glioma patients. J Neurooncol 149:499–510
26. Kondyli M, Larouche V, Saint-Martin C, Ellezam B, Pouliot L, Sinnett D et al (2018) Trametinib for progressive pediatric low-grade gliomas. J Neurooncol 140:435–444
27. Drilon A, Laetsch TW, Kummar S, DuBois SG, Lassen UN, Demetri GD et al (2018) Efficacy of larotrectinib in TRK fusion-positive cancers in adults and children. N Engl J Med 378:731–739
28. D'Arco F, O'Hare P, Dashti F, Lassaletta A, Loka T, Tabori U et al (2018) Volumetric assessment of tumor size changes in pediatric low-grade gliomas: feasibility and comparison with linear measurements. Neuroradiology 60:427–436
29. Fangusaro J, Witt O, Hernáiz Driever P, Bag AK, de Blank P, Kadom N et al (2020) Response assessment in paediatric low-grade glioma: recommendations from the Response Assessment in Pediatric Neuro-Oncology (RAPNO) working group. Lancet Oncol 21:e305–e316

Publisher's Note

Springer Nature remains neutral with regard to jurisdictional claims in published maps and institutional affiliations.

Příloha 2

ORIGINAL ARTICLE - PEDIATRIC NEUROSURGERY

Survival and functional outcomes in paediatric thalamic and thalamopeduncular low grade gliomas

Vladimír Beneš 3rd[1] · Michal Zápotocký[2] · Petr Libý[1] · Jakub Táborský[1] · Jana Blažková Jr[1] · Jana Blažková Sr[3] · David Sumerauer[2] · Adéla Mišove[2] · Ivana Perníková[4] · Martin Kynčl[5] · Lenka Krsková[6] · Miroslav Koblížek[6] · Josef Zámečník[6] · Ondřej Bradáč[1,7] · Michal Tichý[1]

Abstract

Background Childhood thalamopeduncular gliomas arise at the interface of the thalamus and cerebral peduncle. The optimal treatment is total resection but not at the cost of neurological function. We present long-term clinical and oncological outcomes of maximal safe resection.

Methods Retrospective review of prospectively collected data: demography, symptomatology, imaging, extent of resection, surgical complications, histology, functional and oncological outcome.

Results During 16-year period (2005–2020), 21 patients were treated at our institution. These were 13 girls and 8 boys (mean age 7.6 years). Presentation included progressive hemiparesis in 9 patients, raised intracranial pressure in 9 patients and cerebellar symptomatology in 3 patients. The tumour was confined to the thalamus in 6 cases. Extent of resection was judged on postoperative imaging as total (6), near-total (6) and less extensive (9). Surgical complications included progression of baseline neurological status in 6 patients, and 5 of these gradually improved to preoperative status. All tumours were classified as low-grade gliomas. Disease progression was observed in 9 patients (median progression-free survival 7.3 years). At last follow-up (median 6.1 years), all patients were alive, median Lansky score of 90. Seven patients were without evidence of disease, 6 had stable disease, 7 stable following progression and 1 had progressive disease managed expectantly.

Conclusion Paediatric patients with low-grade thalamopeduncular gliomas have excellent long-term functional and oncological outcomes when gross total resection is not achievable. Surgery should aim at total resection; however, neurological function should not be endangered due to excellent chance for long-term survival.

Keywords Childhood glioma · Low-grade astrocytoma · Survival · Extent of resection · Thalamus

Abbreviations

cDNA	Complementary deoxyribonucleic acid
CST	Cortico-spinal tract
DNA	Deoxyribonucleic acid
EOR	Extent of resection
ETV	Endoscopic third ventriculostomy
FLAIR	Fluid-attenuated inversion recovery
GTR	Gross total resection
LGG	Low-grade glioma
MCS	Milan Complexity Scale
MRI	Magnetic resonance imaging
NTR	Near total resection
OS	Overall survival
PCR	Polymerase chain reaction
PFS	Progression-free survival
PR	Partial resection
RNA	Ribonucleic acid
RT PCR	Reverse transcriptase polymerase chain reaction
STR	Subtotal resection

✉ Vladimír Beneš 3rd
vladimir.benes@fnmotol.cz

Extended author information available on the last page of the article

Introduction

Childhood tumours of the thalamic region are rare, representing less than 5% of brain tumour histopathology [6, 8, 14, 39]. They either arise directly at the thalamus or at the junction of thalamus and cerebral peduncle, so-called thalamopeduncular tumours [25]. Historically, surgery for these tumours was more conservative due to proximity of internal capsule, cortico-spinal tract (CST), hypothalamus, mesencephalon and other vital neurovascular structures and was thus deemed very high risk. Progress in neuroimaging allowing detailed presurgical planning, advanced microsurgical techniques and intraoperative neuromonitoring along with image guidance and postoperative care have shifted the balance towards more extensive resection in recent decades [4, 7, 20, 34, 36, 43]. More extensive surgery was associated with acceptable rates of surgical morbidity-mortality and excellent long-term survival especially in low-grade tumours.

Children with low-grade gliomas (LGG) have a very high chance of reaching adulthood, and in case of pilocytic astrocytoma histology, complete cure can be achieved with total resection, usually without the need for adjuvant oncological treatment [40]. In these patients, surgery should aim at maximal safe resection, that is surgery guided by intraoperative neuromonitoring and image guidance, where maintaining preoperative level of function takes precedence over resection extent. The goal of surgery is not a postoperative image where total resection is achieved but the patient is left severely disabled; rather, the goal is stable or improved neurological status regardless of resection extent.

The purpose of this study was to assess our surgical philosophy and strategy of maximal safe resection as described above in children harbouring thalamic and thalamopeduncular LGGs.

Patients and methods

Patient population

Patients treated for thalamic and thalamopeduncular LGG between 2005 and 2020 at our institution were identified in a prospectively collected database. Lesions originating from adjacent structures (optic pathways, hypothalamus, basal ganglia, brainstem, ventricles, pineal region or cerebellum) and merely extending into the thalamus or cerebral peduncle were excluded. Patients treated surgically elsewhere and referred to our tertiary centre for oncological treatment were excluded as well.

Clinical data and outcome assessment

Collected data included basic demography (gender, age) at presentation, duration and type of symptoms, and school attendance. Follow-up visits were scheduled postoperatively at 6 weeks, 3 months, 6 months, 1 year and annually thereafter. Clinical status of the patient was assessed preoperatively and at follow-up visits using the Lansky scale [18]. Current school type, grade and/or highest attained education or current employment was also noted. Neurological status was assessed preoperatively, postoperatively (usually on postoperative day one), at discharge and during follow-up visits. Permanent surgery-related neurological deficit was defined as absent on baseline examination and present at 3 months follow-up. Surgical mortality was defined as any death within 30 days of surgery. At each follow-up visit, patients were also classified according to disease status: complete remission with no residual tumour, stable disease and progressive disease. Disease progression was defined as tumour recurrence after gross-total or near-total resection, progression of residual tumour by more than 25% [10] after subtotal or partial resection or metastatic disease distant from the primary surgery site.

Neuroimaging

Each patient underwent detailed magnetic resonance imaging (MRI) preoperatively. In recent cases, diffusion tensor imaging was also used to assess the course of the CST and other relevant neural pathways (e.g. optic tract). Details noted on MRI included presence of cysts, calcifications, oedema, character of contrast media uptake, extension into surrounding structures and presence of hydrocephalus. For the purpose of preoperative volumetric analysis, the tumour was depicted on T1-weighted gadolinium enhanced, T2-weighted or fluid-attenuated inversion recovery (FLAIR) sequences depending on properties of the tumour. The 3D Slicer software [11] was used to quantify tumour volume on serial axial slices (0.7-mm or 1-mm cuts). Two clinicians (one experienced neurosurgeon not involved in the surgery and one neuroradiologist) blinded to the patient information performed the analysis. If the values differed substantially, a third independent analysis was performed. The final volume was calculated as mean from two most similar values (of the eventual three performed). Identical approach was used to calculate postoperative tumour volume on MRI performed on the first or second postoperative day (no later than 48 h). Extent of resection (EOR) was then calculated using the equation: $100 - (\text{postoperative volume/preoperative volume} \times 100)$ with the result expressed in percentage of resection. EOR

was classified using MRI volumetry as gross-total resection (GTR): no residual tumour on postoperative MRI; near-total resection (NTR): 95–99% resection; subtotal resection (STR): 80–95% resection; and partial resection (PR): less than 80% resection [17]. Surgical complications (e.g. haematoma or ischemia) were also assessed on postoperative MRI. Follow-up MRI was used to evaluate eventual tumour progression as described above.

Surgery

Surgery aimed at achieving GTR whenever deemed feasible and safe. Surgery was performed using standard microsurgical techniques under electrophysiological monitoring and image guidance. Decrease in amplitude ($<50\%$) of somatosensory evoked potentials, significant increase of transcranial threshold stimulation (20% of baseline value), decrease of amplitude ($<50\%$) or change in latency of motor evoked potentials warned the surgeon against pursuing further resection. Further increase in threshold stimulation (50% of baseline value) and/or decrease of amplitude ($<20\%$) was signal for immediate stop of resection. Similarly, direct stimulation of CST using a monopolar electrode was considered safe up to 5 mA. If clear tumour margin could be maintained, resection was pursued unless deterioration of electrophysiology occurred. Care was taken to respect electrophysiological and image-guided presence of descending white matter tracts or eloquent cortical areas. Various surgical approaches were used according to the extent of the tumour. Approach was tailored specifically to the lesion and included transsylvian/pterional, middle-temporal gyrus, transcortical/transventricular, transcallosal/transventricular and supracerebellar-infratentorial with various modifications according to tumour extension. When appropriate, surgery was performed in staged fashion. The complexity of surgery was assessed retrospectively through the Milan Complexity Scale (MCS) [12] according to preoperative MRI images and surgical notes. This scale can evaluate the risk of postoperative neurological worsening after brain tumour surgery according to five parameters: involvement of major brain vessels, posterior fossa location, cranial nerve manipulation, tumour eloquent location and tumour size greater than 4 cm. The resulting sum ranges from 0 to 8 points and higher values have increased risk of postoperative worsening (Table 1).

Hydrocephalus was managed preoperatively by external ventricular drainage, endoscopic third ventriculostomy (ETV) or postoperative shunting as the clinical situation demanded.

Genetic analysis

Diagnostic evaluation to detect LGG-associated molecular alterations was performed in a stepwise manner. Most

Table 1 Milan Complexity Scale (MCS) [12] and the number of patients positive for each variable

Variable	Score	Number of patients (%)
Major brain vessel manipulation[a]		
No	0	
Yes	1	15 (71)
Posterior fossa		
No	0	
Yes	1	9 (43)
Cranial nerve manipulation		
No	0	
Yes	2	7 (33)
Eloquent area[b]		
No	0	
Yes	3	21 (100)
Tumour size		
0–4 cm	0	
4.1 cm +	1	11 (52)
Total score	0–8	Mean score: 5, range 3–8

[a]Major vessels include: internal carotid artery; anterior, middle and posterior cerebral artery; anterior and posterior communicating artery; anterior choroidal artery; ophthalmic artery; vertebral artery; basilar artery; superior, anterior inferior and posterior inferior cerebellar artery; superior sagittal, transverse, sigmoid sinus; internal cerebral veins; vein of Galen

[b]Eloquent areas include motor, sensory, language, visual cortex, hypothalamus, thalamus, internal capsule, brainstem, pineal region

common alterations were detected by direct sequencing from tumour DNA (*BRAF V600E*) or reverse transcriptase-PCR (RT-PCR) cDNA achieved by reverse transcription of tumour RNA (*KIAA1549-BRAF*) as previously described [37]. Wild-type cases were subjected to panel RNA sequencing using ArcherDX Lung panel kit (ArcherDX, CO, USA).

Statistical analysis

The risk for immediate postoperative worsening was compared for MCS scores 0–4 vs. MCS scores 5–8. Comparison of categorical variables was performed using Fisher's exact test. The Kaplan–Meier method was used to estimate the probability of 5-year overall survival (OS) and 5-year progression-free survival (PFS). *p*-value of less than 0.05 was considered significant.

Results

During the study period, 21 patients were treated at our institution, 11 during the last 5 years (Tables 2 and 3). There were 13 girls and 8 boys (mean age 7.6 years; range 1.25–15.9 years). Presentation included progressive hemiparesis in 9 patients

Table 2 Basic characteristics of the study population

Number of patients	21
Male:female	8:13
Mean age (range); years	7.6 (1.25–15.9)
Mean duration of symptoms (range); days	54.2 (0–180)
Location	
Thalamus (bilateral)	6 (2)
Thalamopeduncular	15
Tumour extension	
Tentorial incisura	5
Pineal region	3
Basal ganglia	2
Third ventricle	2
Cerebello-pontine angle	2
Radiological features	
Contrast enhancement	21
Heterogeneous appearance	16
Cystic tumour	16
Calcifications	4
Mean tumour volume (range); cm^3	29 (3.9–96.6)
Hydrocephalus present	14
External ventricular drainage	5
Endoscopic ventriculostomy	8
Eventual shunting	7

(Fig. 1), symptoms of raised intracranial pressure in 9 patients (Fig. 2) and cerebellar symptomatology in 3 patients due to tumour extension into the posterior fossa. Mean symptom duration was 54.2 days (range 0–180). The tumour was confined to the thalamus in 6 patients (bilateral involvement in 2 patients); in 15 patients, simultaneous involvement of the cerebral peduncle was evident. Homogenous appearance was noted in 5 tumours and calcifications in 4 tumours, all but 5 tumours were cystic and all showed evidence of contrast enhancement on MRI. The mean preoperative tumour volume was 29 cm^3 (range 3.9 cm^3–96.6 cm^3). Most common tumour extension was into the tentorial incisura (5 cases), followed by pineal region (3 cases), basal ganglia, third ventricle and cerebello-pontine angle (2 cases each). Diffusion tensor imaging and fibre tractography were utilised in the last 3 patients and showed anteromedial CST displacement in relation to the tumour in two patients and split CST in the last patient (Fig. 3).

Preoperatively, hydrocephalus was present in 14 patients. Initial treatment included temporary external ventricular drainage in 5 patients. Definite hydrocephalus treatment required ETV in 8 patients and eventual shunt implantation in 7 of these patients.

In 2 patients, stereotactic biopsy was performed as a first procedure; both underwent subsequent transcortical/transventricular resection. The most common approach was supracerebellar-infratentorial (12 patients) followed by transcortical/transventricular (4 patients), pterional/transsylvian (3 patients), middle temporal gyrus (1 patient) and transcallosal/transventricular (1 patient). The mean MCS score was 5 points (range 3–8) (Table 1). There was no surgical mortality. Surgical complications included immediate worsening of the postoperative neurological status and Lansky score progression in 6 patients (28.6%); 5 of these returned to preoperative level at 3 months follow-up. The rate of permanent surgical morbidity in this study was thus 4.7%. These complicated patients were distributed evenly across the study period and no relation was found to EOR (GTR/NTR vs. STR/PR: 4/12 vs. 2/9; $p = 0.659$, Fisher's exact test).

Tumour histology revealed LGG in all patients (grade II in 5 patients, all remaining were classified as grade I pilocytic astrocytomas). All tumours were examined for proliferation activity using the Ki67 marker; mean positivity detected was 2.5% (range 0–4%).

Underlying molecular alteration was successfully identified in 17 patients (81%). Majority of patients harboured *KIAA1549-BRAF* fusion ($n = 10$) or *BRAF V600E* mutation ($n = 3$). Receptor tyrosin kinase–associated alteration was uncovered in three patients (*FGFR1*, *NTRK1* and *ROS1*). One patient was diagnosed with germ line *NF1* mutation resulting in neurofibromatosis type 1. Three patients (19%) did not have any alteration revealed due to insufficient tumour tissue ($n = 3$) or negative results of all used tests including RNA sequencing ($n = 1$).

GTR was achieved in 6 patients (28.6%), NTR in 6 patients (28.6%), STR in 5 patients (23.8%) and PR in 4 patients (19%). Mean residual tumour volume was 2.2 cm^3 (range 0 cm^3–9.5 cm^3). Disease progression was observed in 9 patients with a median progression-free survival of 7.3 years: recurrence after NTR in 4 patients and residual tumour progression in 5 patients after STR or PR. All recurrent tumours were asymptomatic and diagnosed on routine follow-up MRI. Additional surgery for tumour progression was performed in 5 patients (1 subsequent GTR), 3 of these received additional chemotherapy and 2 patients received additional chemotherapy only without surgery. Chemotherapy regime included combination of carboplatine and vincristine in 3 patients and vinblastine only in 2 patients. Two patients experienced allergic reaction to carboplatine and this was substituted by cyclophosphamide. No further serious chemotherapy-related adverse events were recorded. The last patient with tumour progression is managed expectantly due to excellent functional status and involvement of eloquent areas. No patient received radiotherapy. At last follow-up (median 6.1 years), all patients were alive, 7 without evidence of disease, 6 with initial residual but stable disease, 7 with stable disease after progression and therapy and one patient as progressive disease managed expectantly (Fig. 4, Table 3).

Table 3 Individual data for each patient

Patient	Gender; age (years)	Symptomatology	Duration (days)	Location	Extension	Preoperative hydrocephalus	Approach	Milan Complexity Scale[12]
1	F; 9.0	Raised ICP	60	Thalamus bilateral	Third ventricle	Yes	Biopsy; transcortical/transventricular	3
2	M; 14.1	Hemiparesis	30	Thalamus (right)		No	Biopsy; transcortical/transventricular	3
3	M; 8.6	Raised ICP	60	Thalamopeduncular (left)		Yes	SCIT	5
4	F; 9.4	Raised ICP	30	Thalamus (left)	Third ventricle	Yes	SCIT	5
5	M; 4.6	Hemiparesis	54	Thalamopeduncular (right)		No	Pterional/transsylvian	6
6	F; 2.7	Hemiparesis	90	Thalamus (left)		No	Transcallosal/transventricular	4
7	F; 5.9	Raised ICP	45	Thalamopeduncular (left)		Yes	SCIT	4
8	F; 12.4	Hemiparesis	90	Thalamopeduncular (left)		Yes	SCIT	4
9	M; 6.1	Hemiparesis	3	Thalamopeduncular (right)		No	Transcortical/transventricular	4
10	M; 4.2	Cerebellar	120	Thalamopeduncular (left)		Yes	SCIT	5
11	F; 15.9	Raised ICP	5	Thalamopeduncular (left)		Yes	SCIT	4
12	F; 5.5 (Fig. 1)	Hemiparesis	21	Thalamus (left)	Basal ganglia	No	Pterional/transsylvian	7
13	F; 11.3	Raised ICP	7	Thalamopeduncular (right)		Yes	Transcortical/transventricular	5
14	F; 9.6	Cerebellar	180	Thalamopeduncular (right)	Tentorial incisura, CP angle	Yes	SCIT	7
15	F; 10.6	Raised ICP	30	Thalamus bilateral	Tentorial incisura, pineal region	Yes	SCIT	6
16	M; 1.3	Raised ICP	0	Thalamopeduncular (left)	Tentorial incisura, pineal region	Yes	SCIT	6
17	M; 7.4 (Fig. 2)	Raised ICP	7	Thalamopeduncular (left)		Yes	SCIT	4
18	F; 3.4	Hemiparesis	7	Thalamopeduncular (right)	CP angle	No	SCIT	8
19	M; 5.6	Hemiparesis	180	Thalamopeduncular (left)	Basal ganglia	Yes	Middle temporal gyrus	7
20	F; 3.3	Hemiparesis	60	Thalamopeduncular (right)	Tentorial incisura, sellar region	No	Pterional/transsylvian	7
21	F; 9.7 (Fig. 3)	Cerebellar	60	Thalamopeduncular (right)	Tentorial incisura, pineal region	Yes	SCIT	8

Table 3 (continued)

Patient	Resection extent	Permanent hydrocephalus management	Histology	Molecular alteration	Postoperative progression	Recurrence (months)	Recurrence management	Oncological status	Follow-up (months)	Lansky score
1	PR	ETV, VPS	Grade 1	*BRAF V600E*	Transient			Stable initial residual	187.5	100
2	GTR		Grade 2	Insufficient material				No evidence of disease	101.8	90
3	STR	ETV, VPS	Grade 2	Receptor tyrosin kinase (*NTRK1* fusion)				Stable initial residual	116.5	100
4	PR	ETV	Grade 1	*BRAF V600E*		84.7	Observation, stable afterwards	Stable after progression/therapy	118.3	90
5	STR		Grade 1	*KIAA1549-BRAF* fusion	Permanent	91.1	CHT	Stable after progression/therapy	116.4	90
6	NTR		Grade 2	Insufficient material		2.9	Surgery, CHT	Stable after progression/therapy	108.3	70
7	STR	ETV, VPS	Grade 1	Germ line *NF-1* mutation		11.2	Surgery, CHT	Stable after progression/therapy	110.8	90
8	PR	ETV, VPS	Grade 2	*BRAF V600E*				Stable initial residual	93.1	100
9	STR		Grade 1	*KIAA1549-BRAF* fusion		5.9	CHT	Stable after progression/therapy	93.6	100
10	GTR		Grade 1	*KIAA1549-BRAF* fusion	Transient			No evidence of disease	90.3	90
11	GTR	ETV, VPS	Grade 1	negative				No evidence of disease	73.2	100
12	GTR		Grade 1	*KIAA1549-BRAF* fusion				No evidence of disease	62.9	100
13	NTR		Grade 2	Insufficient material				Stable initial residual	72.8	100
14	NTR	ETV, VPS	Grade 1	*KIAA1549-BRAF* fusion		22.3	Surgery (GTR)	No evidence of disease	63.6	90
15	PR		Grade 1	*KIAA1549-BRAF* fusion		2.66	Surgery	Stable after progression/therapy	46.5	100
16	NTR	ETV, VPS	Grade 1	*KIAA1549-BRAF* fusion	Transient			Stable initial residual	33.3	70
17	GTR		Grade 1	Receptor tyrosin kinase (*FGFR1* fusion)				No evidence of disease	23.0	100
18	NTR		Grade 1	*KIAA1549-BRAF* fusion		6.5	Observation	Observed progression	9.3	90
19	STR		Grade 1	*KIAA1549-BRAF* fusion				Stable initial residual	3.2	90
20	NTR		Grade 1	Receptor tyrosin kinase (*ROS1* fusion)	Transient	2.0	Surgery, CHT	Stable after progression/therapy	5.1	90
21	GTR		Grade 1	*KIAA1549-BRAF* fusion	Transient			No evidence of disease	5.1	80

F female, *M* male, *ICP* intracranial pressure, *SCIT* supracerebellar infratentorial, *PR* partial resection, *STR* subtotal resection, *NTR* near-total resection, *GTR* gross total resection, *ETV* endoscopic third ventriculostomy, *VPS* ventriculoperitoneal shunt, *CHT* chemotherapy

Fig. 1 A 5-year-old girl presenting with hemiparesis. Preoperative magnetic resonance imaging depicts tumour of the left thalamus extending into the basal ganglia. **A** Preoperative T2-sequences in the axial plane, **D** corresponding postoperative image. Contrast-enhanced preoperative images in the sagittal (**B**) and coronal planes (**C**) and corresponding postoperative images (**E**, **F**) show gross total resection via the pterional/transsylvian approach
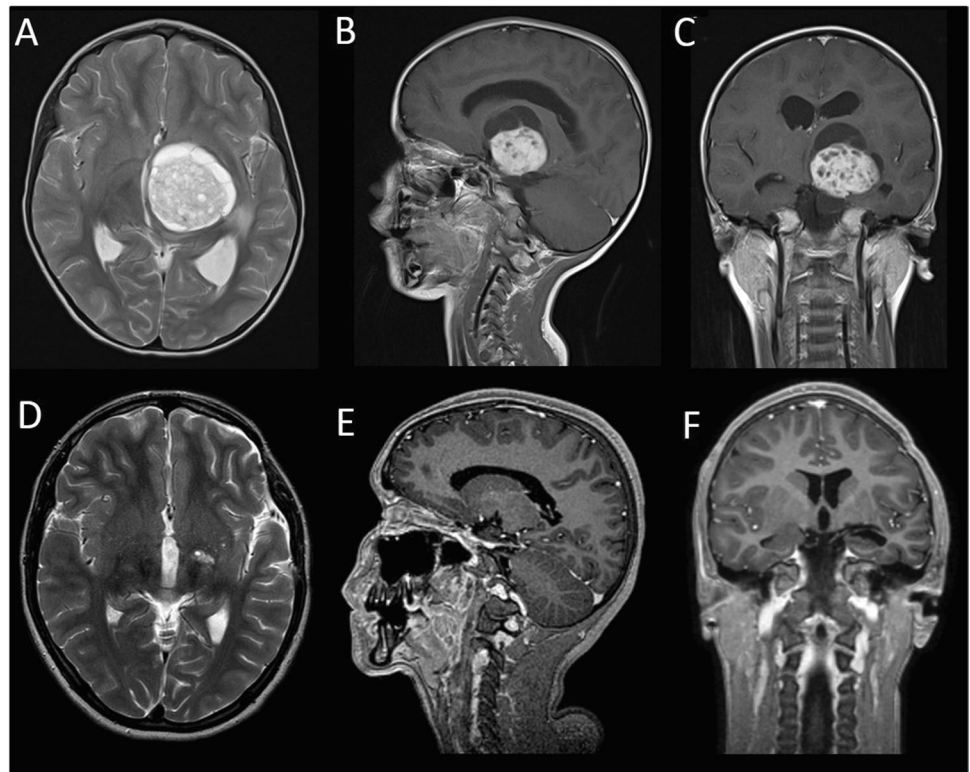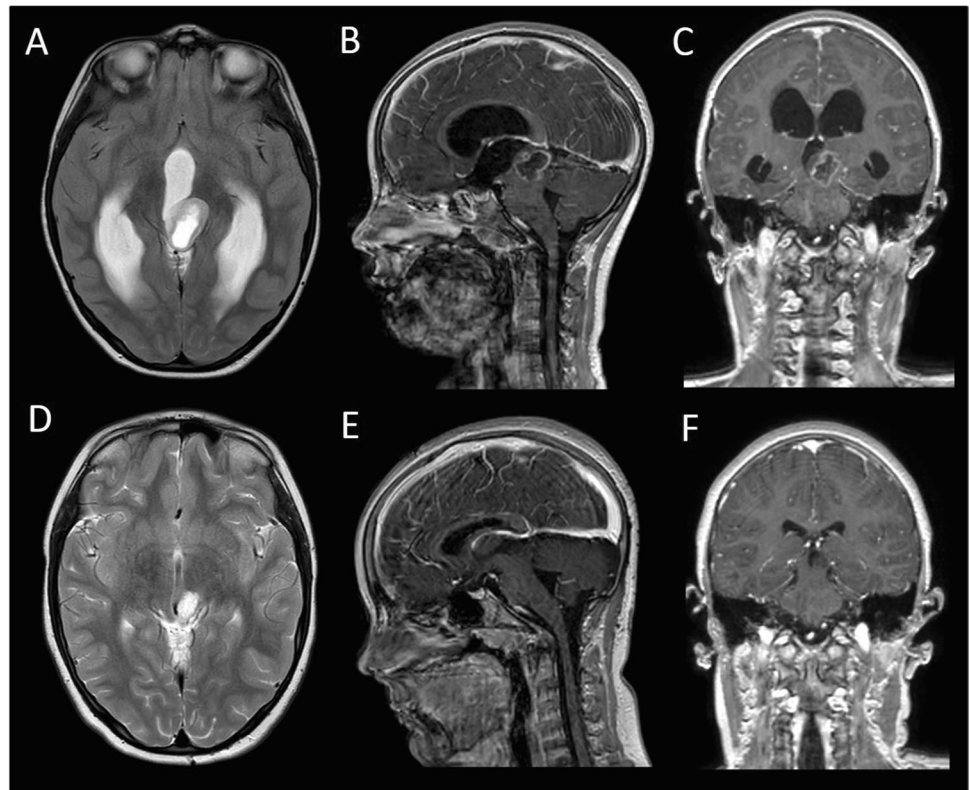

Fig. 2 A 7-year-old boy presenting with raised intracranial pressure due to aqueduct obstruction. Preoperative magnetic resonance (**A–C**) shows solid-cystic tumour with peripheral contrast enhancement (**B**, **C**). Gross total resection was achieved via supracerebellar-infratentorial approach (**D–F**)
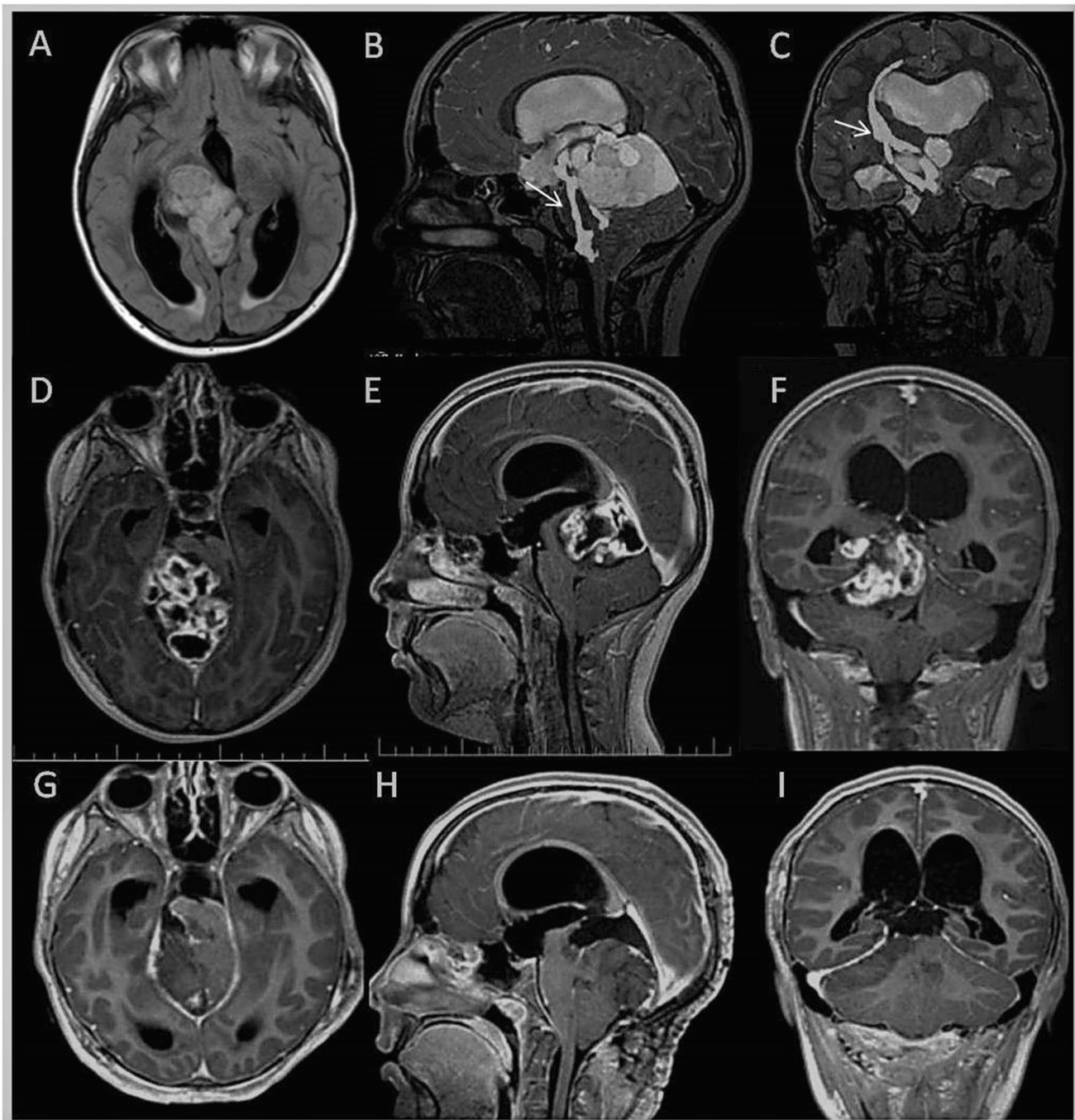
Fig. 3 A 9-year-old girl presenting with cerebellar symptomatology. Preoperative magnetic resonance imaging depicts tumour originating in the right thalamus (**A** axial fluid attenuated inversion recovery image), the course of cortico-spinal tract (arrow on B, C; T2-sequences with diffusion tensor imaging) in relation to the tumour. Preoperative 3D Turbo Field Echo sequences with contrast enhancement of the multicystic tumour (**D**, **E**, **F**) and corresponding postoperative imaging confirming gross total resection (**G**, **H**, **I**)

Last median Lansky score was 90 (70–100), 10 patients are attending elementary school (4 have individual study plans), 5 have either finished or are attending high-school, one is studying university and one is employed; the last 4 patients have yet to reach school age.

Statistical analysis

Comparing patients with MCS scores 0–4 (1/8 patients with immediate complication) to patients with MCS scores 5–8 (5/13 patients with immediate complication) did not reach
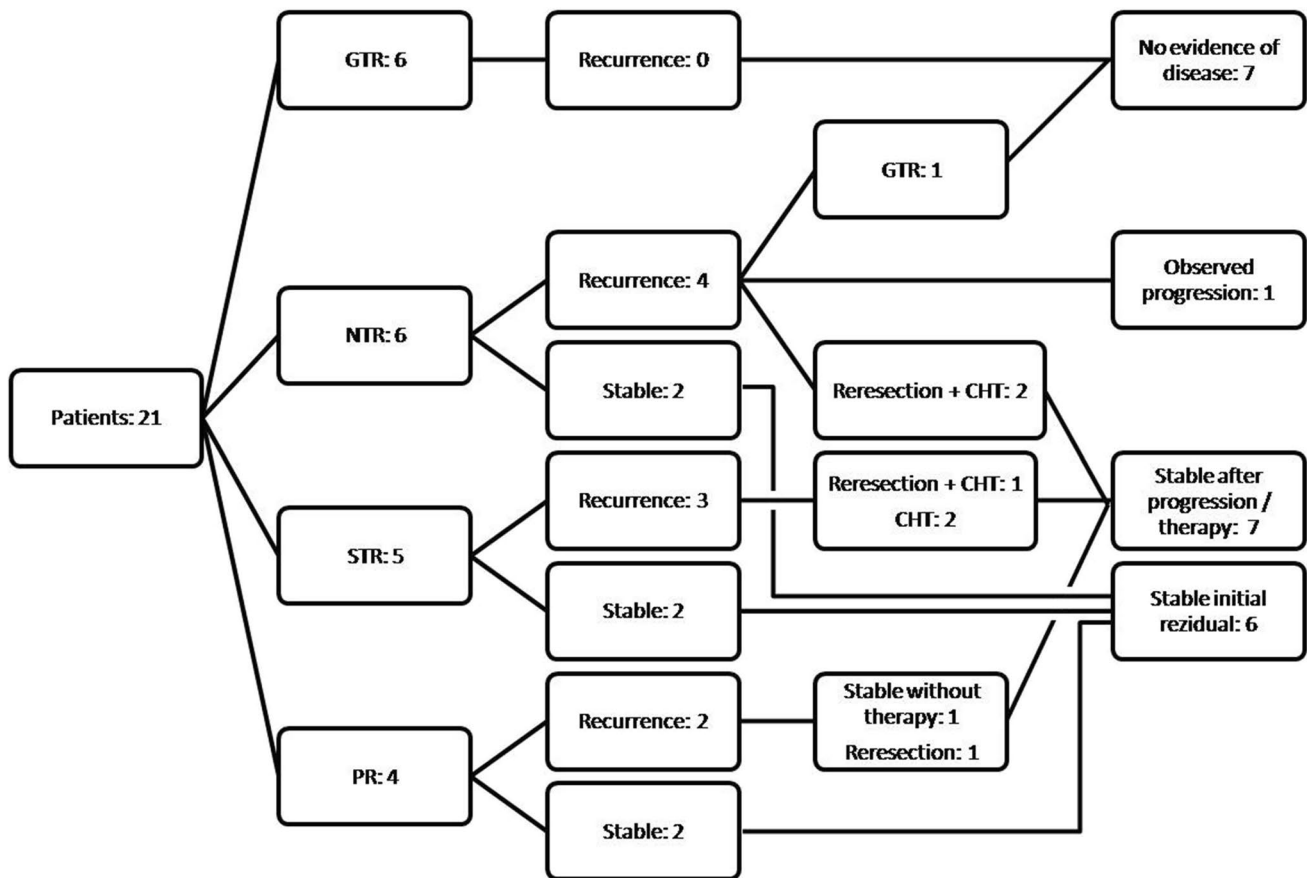
Fig. 4 Flowchart depicting extent of resection, recurrence and additional therapy. GTR, gross total resection; NTR, near total resection; STR, subtotal resection; PR, partial resection; CHT, chemotherapy

statistical significance ($p=0.336$, Fisher's exact test). Five-year OS in this patient cohort was 100%, and 5-year PFS was 64% (Fig. 5). No patient who underwent initial GTR (6 patients) experienced disease progression in comparison to 9/15 patients with less extensive EOR ($p=0.019$, Fisher's exact test).

Discussion

Natural history of paediatric LGGs is rather favourable and children have excellent survival prognosis in comparison to adults. OS rates at 10 and 20 years range from 80 to 90% [1, 13, 31] and adult surviving patients have low probability of glioma-related death [1]. Contrary to their adult counterparts [16, 28, 41], paediatric LGGs very rarely undergo malignant transformation in adulthood [1, 21, 33]. Furthermore, pilocytic histology was identified as a favourable prognostic factor in comparison to non-pilocytic histology [1, 33] and pilocytic astrocytomas have a very low mortality rate (3.1%) [30]. Thus, children with pilocytic astrocytomas (and LGGs) have a very high probability of reaching advanced adulthood and not succumbing to their glioma. All these facts have to

be factored into a treatment plan which should aim at maximising tumour control and minimising treatment-related complications and toxicity.

The cornerstone of treatment is surgery. Surgery obtains representative histological samples, relieves tumour-associated mass effect and addresses hydrocephalus which is often present due to aqueduct obstruction. The location of thalamopeduncular astrocytomas is highly eloquent and surgically challenging. The borders of the thalamus comprise hypothalamus (inferior), third ventricle (medial), lateral ventricle and stria medullaris (superior), posterior limb of internal capsule (lateral), foramen of Monro (anterior) and posterior commissure (posterior). These borders also define thalamic surfaces that can be reached through transcisternal or transcallosal/transverntricular approaches avoiding the need to transgress brain parenchyma: the posteriorly projecting cisternal surface through modifications of supracerebellar infra-/transtentorial or posterior interhemispheric transtentorial subsplenial approach; the lateral-ventricular and velar surfaces through the anterior interhemispheric transcallosal approach; the third ventricular surface through the contralateral supracerebellar suprapineal approach. These accessible
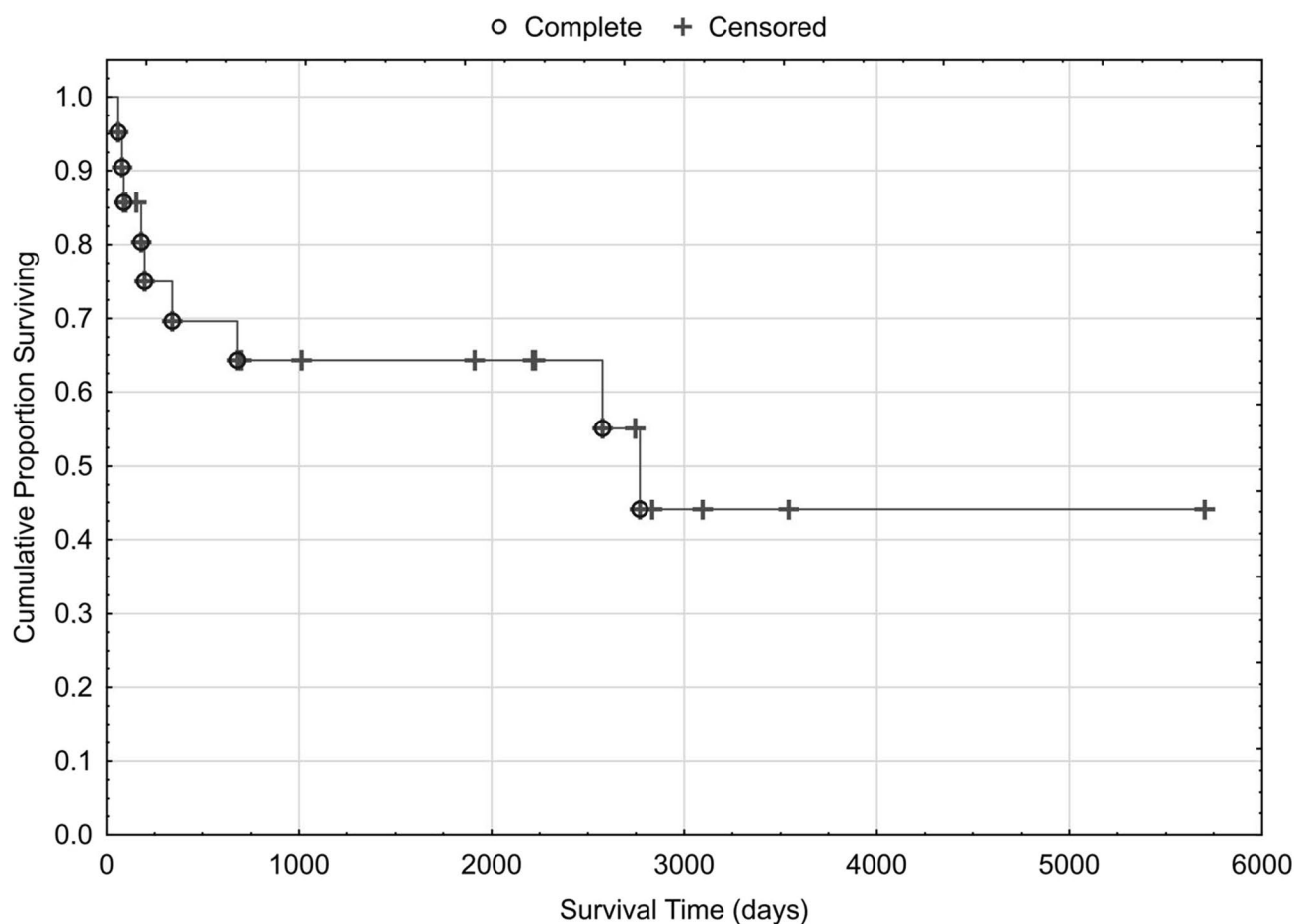
Fig. 5 Progression-free survival of the patient cohort using the Kaplan–Meier method

thalamic surfaces allow the surgeon to safely reach most tumours confined within the thalamus and in effect dictate the approach according to the closest surface to the lesion [34]. Alternatively, thalamus can be divided into six segments and each of these can be reached by a corresponding approach: anteroinferior (orbitozygomatic approach), medial (anterior ipsilateral transcallosal approach), lateral (anterior contralateral transcallosal approach), posterosuperior (posterior transcallosal approach), lateral posteroinferior (parietooccipital transventricular approach) and medial posteroinferior (supracerebellar-infratentorial approach) [27].

Furthermore, thalamopeduncular astrocytomas tend to expand outwardly and compress surrounding eloquent areas (e.g. basal ganglia, CST, hypothalamus, optic pathways and aqueduct) or stretch critical neurovascular structures (e.g. optic nerve, oculomotor nerve, deep venous system, posterior cerebral artery). Extension into the tentorial incisura and cerebello-pontine angle endangers additional cranial nerves and cerebral vessels. Intraoperative injury is more likely because these structures are sometimes at their functional limit (particularly the oculomotor nerve) and any

additional manipulation can lead to mechanical or vascular damage. These pitfalls are very relevantly reflected in the Milan Complexity Scale [12]. Indeed 13 of our patients scored 5 or more points and had higher probability of immediate postoperative worsening, although this difference did not reach statistical significance, due to small sample size. Fortunately, all but one postoperative decline in functional status improved at follow-up with time and physiotherapy. Other studies also confirm this extraordinary plasticity of children's nervous system [2, 7] where postoperative deficits (although likely to occur after surgery for midline tumours) usually improve during follow-up.

Detailed knowledge of the relevant anatomy, intraoperative image guidance, neuromonitoring of somatosensory and motor evoked potentials and cortical as well as CST mapping are prerequisites for safe surgery in and around the thalamic region. Several approaches to the thalamus and cerebral peduncles are feasible [3, 8, 24, 25, 35]; however, no approach is universal and needs to be adjusted individually. Recently, preoperative diffusion tensor imaging of CST was reported to analyse its displacement [4, 5, 22]. The direction

of CST displacement varies widely; anterior or anterolateral being the most common [4, 5, 20, 22]. Additionally, the location of the optic tract and visual pathway needs to be considered. Eventual extracerebral extension of the lesion can also guide the approach. Thus, preoperative approach planning should take into account (among other factors) displacement of CST, visual pathway and extracerebral projection of the tumour (Table 4). Despite using fibre tractography in our last cases only, we did not encounter increased risk of postoperative decline in the earlier part of the study period, probably due to careful approach selection based on known anatomical landmarks and surgeon's familiarity with the approach.

Majority of tumours (12) were addressed by the supracerebellar-infratentorial approach which is familiar to most neurosurgeons, keeps anatomical orientation relatively simple and allows the surgeon to easily reach parts of the tumour extending into the incisura, posterior fossa, cerebello-pontine angle and with tentorial section into supratentorial space.

Table 4 Simplified approaches to thalamic and thalamopeduncular tumours

Tumour confined to the thalamus
- Reaches (or closest) thalamic surface
o Lateral ventricle
■ Transcallosal/transventricular
■ Transcortical/transventricular
o Third ventricle
■ Contralateral supracerebellar suprapineal
o Cisternal
■ Supracerebellar infra-/transtentorial
■ Posterior interhemispheric transtentorial subsplenial
- Thalamic region
o Anteroinferior
■ Orbitozygomatic
o Medial
■ Anterior ipsilateral transcallosal
o Lateral
■ Anterior contralateral transcallosal
o Posterosuperior
■ Posterior transcallosal
o Lateral posteroinferior
■ Parietooccipital transventricular
o Medial posteroinferior
■ Supracerebellar infratentorial
Extracerebral extension
- Tentorial incisura
o Supracerebellar-infratentorial
o Retrosigmoid extension if cerebello-pontine angle involved
o Transtentorial if supratentorial extension
- Anterior
o Pterional/transsylvian
- Lateral
o Middle temporal gyrus

Displacement of corticospinal tract and visual pathway depicted on diffusion tensor imaging needs to be considered

Following gravity retraction of the cerebellum, and elevation of the tentorium with retention sutures, a wide corridor is developed which allows ample space for tumour dissection. Deep venous system is usually dislocated superiorly, posterior cerebral arteries laterally and superior cerebellar arteries caudally. These structures (along with the fourth nerve at the edge of the tentorium) need to be identified early and vigorously protected. Furthermore, as tumour dissection and resection proceeds, cerebral peduncles and thalami are identified and tumour can be removed at this location under electrophysiological monitoring. This approach is optimal to use if the CST is displaced anteriorly or anterolaterally. On the other hand, even a discrete presence of normal tissue dorsal to the tumour identifiable on preoperative MRI suggests the course of eloquent tracts and if no dorsal tumour extension outside of the peduncle or thalamus is clearly visible, other surgical route should be chosen according to the principle discussed above.

The rates of gross total resection of thalamic tumours vary in the literature from 0 [15] to 81% [14] or 92% if NTR is included as well [34]. Such a wide range of reported GTR can be attributed to GTR definition criteria, combined reporting of both low- and high-grade tumours, inclusion of bilateral lesions, surgeon's experience, choice of surgical approach, intraoperative deterioration of electrophysiological monitoring and other factors [7, 25, 29, 34, 43]. Our rate of GTR of 28.6% and combined GTR/NTR rate of 57.2% falls in line with the literature. The main reason for less extensive resection in this series is our philosophy where postoperative function has priority over resection extent, particularly in the setting of low-grade tumours. The decision on EOR is modified by the surgeon during surgery based mainly on clearly defined tumour margins and electrophysiological monitoring. Taking into consideration deterioration of somatosensory and motor evoked potentials and proximity of CST by direct stimulation, we were able to prevent long-term postoperative neurological decline in all but one patient. Of note, in this and another patient, further resection was abandoned when direct subcortical stimulation of CST showed its proximity (5 mA positive response) and no clear tumour margin could be identified. This is contrary to our attitude to high-grade lesions (such as anaplastic ependymoma) where the difference between GTR and STR has significant implications for survival [26, 42] more extensive surgery and even severe postoperative deficit is acceptable given the discussed plasticity of children's nervous system. With this conservative approach, we were able to achieve a 4.7% rate of permanent surgery-related neurological deficit and median Lansky score of 90, which both compares favourably to contemporary literature [4, 7, 20, 25, 38, 43]. It is necessary to emphasise that no significant difference was found between surgical morbidity and EOR; however, only GTR proved to be significant for preventing disease recurrence and achieving complete cure.

The advances in oncological therapy and biological treatment further support our surgical philosophy of putting

quality of life first. Many residual tumours can be observed with serial MRI, and upon progression or clinical manifestation, further surgery and/or oncological therapy can be considered depending on tumour location and patient functional status. Long-term tumour control with modern agents can be achieved without significant treatment-related side effects [9]. In fact, no patient in this series experienced serious chemotherapy-related morbidity. Radiotherapy was avoided completely in this patient cohort, considering its deleterious long-term effects on developing brain.

Molecular genetics evaluation of the tumour tissue provided important insight into the biology of thalamopeduncular LGGs. Histologically, the majority of tumours were classified as pilocytic astrocytoma or diffuse astrocytoma. This was reflected by the distribution of molecular alteration with *BRAF* alterations being the most prevalent; *KIAA1549-BRAF* a *BRAF V600E* accounted for 76% molecular changes. These findings correlated with previously published evidence of alterations among LGGs located within midline brain structures [32, 44]. In our cohort, molecularly confirmed thalamopeduncular LGGs harboured excellent prognosis with no patient succumbing to the disease with the median time of follow-up of 6.1 years. This underscored the need for complex histopathological and molecular evaluations confirming the diagnosis of LGG. Our data support the strategy of less aggressive approach in the LGG of midline locations where incomplete resection is acceptable in exchange for better neurological outcome with maintained excellent prognosis. Similarly, approaches for progressive cases should account for radiation sparing therapies in order to avoid deleterious long-term side effects. Moreover, molecular testing is critical to identify targets for novel targeted therapies that offer further options for non-surgical therapies with acceptable toxicities. In our cohort, no patient was treated with any of the targeted agents (yet), but *KIAA1549-BRAF* cases would be suitable candidates for the use of MEK inhibitors, *BRAF V600E* for BRAF inhibitors in case of tumour progression and/or clinical manifestation [19, 23].

Limitations of this study must be kept in mind. This is a single-centre retrospective analysis spanning many years and with a limited number of patients. Although the basic surgical strategy remained unchanged, unknown bias could have been introduced. Multicentre collaboration and large sample size would address most of these shortcomings and help identify other factors relevant to surgical morbidity and oncological prognosis.

Conclusion

Childhood thalamopeduncular low-grade astrocytomas can be treated surgically with acceptable extent of resection and surgery-related permanent complications. Due to their indolent biological course and long-term survival, maximum emphasis should be placed on postoperative quality of life. Aggressive treatment endangering function should be avoided since residual/recurrent tumours can be safely managed expectantly, surgically resected or controlled with modern oncological therapy; however, only GTR offers the best chance of achieving complete cure.

Declarations

References

1. Bandopadhayay P, Bergthold G, London WB, Goumnerova LC, Morales La Madrid A, Marcus KJ, Guo D, Ullrich NJ, Robison NJ, Chi SN et al (2014) Long-term outcome of 4,040 children diagnosed with pediatric low-grade gliomas: an analysis of the Surveillance Epidemiology and End Results (SEER) database. Pediatr Blood Cancer 61:1173–1179. https://doi.org/10.1002/pbc.24958

2. Baroncini M, Vinchon M, Minéo JF, Pichon F, Francke JP, Dhellemmes P (2007) Surgical resection of thalamic tumors in children: approaches and clinical results. Childs Nerv Syst 23:753–760. https://doi.org/10.1007/s00381-007-0299-4

3. Bilginer B, Narin F, Işıkay I, Oguz KK, Söylemezoglu F, Akalan N (2014) Thalamic tumors in children. Childs Nerv Syst 30:1493–1498. https://doi.org/10.1007/s00381-014-2420-9

4. Broadway SJ, Ogg RJ, Scoggins MA, Sanford R, Patay Z, Boop FA (2011) Surgical management of tumors producing the thalamopeduncular syndrome of childhood. J Neurosurg Pediatr 7:589–595. https://doi.org/10.3171/2011.4.Peds119

5. Celtikci E, Celtikci P, Fernandes-Cabral DT, Ucar M, Fernandez-Miranda JC, Borcek AO (2017) High-definition fiber tractography in evaluation and surgical planning of thalamopeduncular

pilocytic astrocytomas in pediatric population: case series and review of literature. World Neurosurg 98:463–469. https://doi.org/10.1016/j.wneu.2016.11.061

6. Cheek WR, Taveras JM (1966) Thalamic tumors. J Neurosurg 24:505–513. https://doi.org/10.3171/jns.1966.24.2.0505

7. Cinalli G, Aguirre DT, Mirone G, Ruggiero C, Cascone D, Quaglietta L, Aliberti F, Santi SD, Buonocore MC, Nastro A et al (2018) Surgical treatment of thalamic tumors in children. J Neurosurg Pediatr 21:247–257. https://doi.org/10.3171/2017.7.Peds16463

8. Cuccia V, Monges J (1997) Thalamic tumors in children. Childs Nerv Syst 13: 514–520; discussion 521 https://doi.org/10.1007/s003810050128

9. Douw L, Klein M, Fagel SS, van den Heuvel J, Taphoorn MJ, Aaronson NK, Postma TJ, Vandertop WP, Mooij JJ, Boerman RH et al (2009) Cognitive and radiological effects of radiotherapy in patients with low-grade glioma: long-term follow-up. Lancet Neurol 8:810–818. https://doi.org/10.1016/s1474-4422(09)70204-2

10. Fangusaro J, Witt O, Hernáiz Driever P, Bag AK, de Blank P, Kadom N, Kilburn L, Lober RM, Robison NJ, Fisher MJ et al (2020) Response assessment in paediatric low-grade glioma: recommendations from the Response Assessment in Pediatric Neuro-Oncology (RAPNO) working group. Lancet Oncol 21:e305–e316. https://doi.org/10.1016/s1470-2045(20)30064-4

11. Fedorov A, Beichel R, Kalpathy-Cramer J, Finet J, Fillion-Robin JC, Pujol S, Bauer C, Jennings D, Fennessy F, Sonka M et al (2012) 3D Slicer as an image computing platform for the Quantitative Imaging Network. Magn Reson Imaging 30:1323–1341. https://doi.org/10.1016/j.mri.2012.05.001

12. Ferroli P, Broggi M, Schiavolin S, Acerbi F, Bettamio V, Caldiroli D, Cusin A, La Corte E, Leonardi M, Raggi A et al (2015) Predicting functional impairment in brain tumor surgery: the Big Five and the Milan Complexity Scale. Neurosurg Focus 39:E14. https://doi.org/10.3171/2015.9.Focus15339

13. Gunny RS, Hayward RD, Phipps KP, Harding BN, Saunders DE (2005) Spontaneous regression of residual low-grade cerebellar pilocytic astrocytomas in children. Pediatr Radiol 35:1086–1091. https://doi.org/10.1007/s00247-005-1546-z

14. Hirose G, Lombroso CT, Eisenberg H (1975) Thalamic tumors in childhood. Clinical, laboratory, and therapeutic considerations. Arch Neurol 32:740–744. https://doi.org/10.1001/archneur.1975.00490530062005

15. Hoffman HJ, Soloniuk DS, Humphreys RP, Drake JM, Becker LE, De Lima BO, Piatt JH Jr (1993) Management and outcome of low-grade astrocytomas of the midline in children: a retrospective review. Neurosurgery 33:964–971. https://doi.org/10.1227/00006123-199312000-00002

16. Johnson DR, Brown PD, Galanis E, Hammack JE (2012) Pilocytic astrocytoma survival in adults: analysis of the Surveillance, Epidemiology, and End Results Program of the National Cancer Institute. J Neurooncol 108:187–193. https://doi.org/10.1007/s11060-012-0829-0

17. Karschnia P, Vogelbaum MA, van den Bent M, Cahill DP, Bello L, Narita Y, Berger MS, Weller M, Tonn JC (2021) Evidence-based recommendations on categories for extent of resection in diffuse glioma. Eur J Cancer 149:23–33. https://doi.org/10.1016/j.ejca.2021.03.002

18. Lansky SB, List MA, Lansky LL, Ritter-Sterr C, Miller DR (1987) The measurement of performance in childhood cancer patients. Cancer 60:1651–1656. https://doi.org/10.1002/1097-0142(19871001)60:7%3c1651::aid-cncr2820600738%3e3.0.co;2-j

19. Lassaletta A, Zapotocky M, Mistry M, Ramaswamy V, Honnorat M, Krishnatry R, Guerreiro Stucklin A, Zhukova N, Arnoldo A, Ryall S et al (2017) Therapeutic and prognostic implications of BRAF V600E in pediatric low-grade gliomas. J Clin Oncol 35:2934–2941. https://doi.org/10.1200/jco.2016.71.8726

20. Lee RP, Foster KA, Lillard JC, Klimo P Jr, Ellison DW, Orr B, Boop FA (2017) Surgical and molecular considerations in the treatment of pediatric thalamopeduncular tumors. J Neurosurg Pediatr 20:247–255. https://doi.org/10.3171/2017.4.Peds16668

21. Mistry M, Zhukova N, Merico D, Rakopoulos P, Krishnatry R, Shago M, Stavropoulos J, Alon N, Pole JD, Ray PN et al (2015) BRAF mutation and CDKN2A deletion define a clinically distinct subgroup of childhood secondary high-grade glioma. J Clin Oncol 33:1015–1022. https://doi.org/10.1200/jco.2014.58.3922

22. Moshel YA, Link MJ, Kelly PJ (2007) Stereotactic volumetric resection of thalamic pilocytic astrocytomas. Neurosurgery 61:66–75; discussion 75 Doi https://doi.org/10.1227/01.neu.0000279725.13521.a3

23. Nobre L, Zapotocky M, Ramaswamy V, Ryall S, Bennett J, Alderete D, Balaguer Guill J, Baroni L, Bartels U, Bavle A et al (2020) Outcomes of BRAF V600E pediatric gliomas treated with targeted BRAF inhibition. JCO Precis Oncol 4 https://doi.org/10.1200/po.19.00298

24. Ozek MM, Türe U (2002) Surgical approach to thalamic tumors. Childs Nerv Syst 18:450–456. https://doi.org/10.1007/s00381-002-0608-x

25. Puget S, Crimmins DW, Garnett MR, Grill J, Oliveira R, Boddaert N, Wray A, Lelouch-Tubiana A, Roujeau T, Di Rocco F et al (2007) Thalamic tumors in children: a reappraisal. J Neurosurg 106:354–362. https://doi.org/10.3171/ped.2007.106.5.354

26. Ramaswamy V, Hielscher T, Mack SC, Lassaletta A, Lin T, Pajtler KW, Jones DT, Luu B, Cavalli FM, Aldape K et al (2016) Therapeutic impact of cytoreductive surgery and irradiation of posterior fossa ependymoma in the molecular era: a retrospective multicohort analysis. J Clin Oncol 34:2468–2477. https://doi.org/10.1200/jco.2015.65.7825

27. Rangel-Castilla L, Spetzler RF (2015) The 6 thalamic regions: surgical approaches to thalamic cavernous malformations, operative results, and clinical outcomes. J Neurosurg 123:676–685. https://doi.org/10.3171/2014.11.Jns14381

28. Rees J, Watt H, Jäger HR, Benton C, Tozer D, Tofts P, Waldman A (2009) Volumes and growth rates of untreated adult low-grade gliomas indicate risk of early malignant transformation. Eur J Radiol 72:54–64. https://doi.org/10.1016/j.ejrad.2008.06.013

29. Renedo D, Ferraro F, Johnson AR, Argañaraz R, Giovannini S, Zabala JP, Zemma E, Mantese B (2021) Thalamic tumors in children: case series from our institution and literature review. Childs Nerv Syst 37:457–463. https://doi.org/10.1007/s00381-020-04830-0

30. Renzi S, Michaeli O, Ramaswamy V, Huang A, Stephens D, Maguire B, Tabori U, Bouffet E, Bartels U (2020) Causes of death in pediatric neuro-oncology: the sickkids experience from 2000 to 2017. J Neurooncol 149:181–189. https://doi.org/10.1007/s11060-020-03590-w

31. Rozen WM, Joseph S, Lo PA (2008) Spontaneous regression of low-grade gliomas in pediatric patients without neurofibromatosis. Pediatr Neurosurg 44:324–328. https://doi.org/10.1159/000134925

32. Ryall S, Zapotocky M, Fukuoka K, Nobre L, Guerreiro Stucklin A, Bennett J, Siddaway R, Li C, Pajovic S, Arnoldo A et al (2020) Integrated molecular and clinical analysis of 1,000 pediatric low-grade gliomas. Cancer Cell 37:569-583.e565. https://doi.org/10.1016/j.ccell.2020.03.011

33. Ryu HH, Jung TY, Lee GJ, Lee KH, Jung SH, Jung S, Baek HJ (2015) Differences in the clinical courses of pediatric and adult pilocytic astrocytomas with progression: a single-institution study. Childs Nerv Syst 31:2063–2069. https://doi.org/10.1007/s00381-015-2887-z

34. Serra C, Türe H, Yaltırık CK, Harput MV, Türe U (2020) Microneurosurgical removal of thalamic lesions: surgical results and considerations from a large, single-surgeon consecutive series. J Neurosurg: 1-11 https://doi.org/10.3171/2020.6.Jns20524

35. Smrčka M, Brichtová E, Mackerle Z, Juráň V, Přibáň V (2015) Surgical approaches to thalamic tumors. Cesk Slov Neurol N 78:172–180

36. Steinbok P, Gopalakrishnan CV, Hengel AR, Vitali AM, Poskitt K, Hawkins C, Drake J, Lamberti-Pasculli M, Ajani O, Hader W et al (2016) Pediatric thalamic tumors in the MRI era: a Canadian perspective. Childs Nerv Syst 32:269–280. https://doi.org/10.1007/s00381-015-2968-z

37. Tian Y, Rich BE, Vena N, Craig JM, Macconaill LE, Rajaram V, Goldman S, Taha H, Mahmoud M, Ozek M et al (2011) Detection of KIAA1549-BRAF fusion transcripts in formalin-fixed paraffin-embedded pediatric low-grade gliomas. J Mol Diagn 13:669–677. https://doi.org/10.1016/j.jmoldx.2011.07.002

38. Upadhyaya SA, Koschmann C, Muraszko K, Venneti S, Garton HJ, Hamstra DA, Maher CO, Betz BL, Brown NA, Wahl D et al (2017) Brainstem low-grade gliomas in children-excellent outcomes with multimodality therapy. J Child Neurol 32:194–203. https://doi.org/10.1177/0883073816675547

39. Villarejo F, Amaya C, Pérez Díaz C, Pascual A, Alvarez Sastre C, Goyenechea F (1994) Radical surgery of thalamic tumors in children. Childs Nerv Syst 10:111–114. https://doi.org/10.1007/bf00302774

40. Wisoff JH, Sanford RA, Heier LA, Sposto R, Burger PC, Yates AJ, Holmes EJ, Kun LE (2011) Primary neurosurgery for pediatric low-grade gliomas: a prospective multi-institutional study from the Children's Oncology Group. Neurosurgery 68: 1548–1554; discussion 1554–1545 Doi https://doi.org/10.1227/NEU.0b013e318214a66e

41. Youland RS, Brown PD, Giannini C, Parney IF, Uhm JH, Laack NN (2013) Adult low-grade glioma: 19-year experience at a single institution. Am J Clin Oncol 36:612–619. https://doi.org/10.1097/COC.0b013e31825d580a

42. Zapotocky M, Beera K, Adamski J, Laperierre N, Guger S, Janzen L, Lassaletta A, Figueiredo Nobre L, Bartels U, Tabori U et al (2019) Survival and functional outcomes of molecularly defined childhood posterior fossa ependymoma: cure at a cost. Cancer 125:1867–1876. https://doi.org/10.1002/cncr.31995

43. Zattra CM, Broggi M, Schiavolin S, Schiariti M, Acerbi F, Esposito S, de Laurentis C, Broggi G, Ferroli P (2021) Surgical outcome and indicators of postoperative worsening in intra-axial thalamic and posterior fossa pediatric tumors: preliminary results from a single tertiary referral center cohort. Interdisciplinary Neurosurgery 24:101054. https://doi.org/10.1016/j.inat.2020.101054

44. Zhang J, Wu G, Miller CP, Tatevossian RG, Dalton JD, Tang B, Orisme W, Punchihewa C, Parker M, Qaddoumi I et al (2013) Whole-genome sequencing identifies genetic alterations in pediatric low-grade gliomas. Nat Genet 45:602–612. https://doi.org/10.1038/ng.2611

Comments This manuscript describes a series of 21 children with thalamic and thalamopeduncular low grade gliomas treated between 2005 and 2020. The authors provide a good description of their patients and their surgical technique, emphasising their choice of operative approach, their use of adjunctive methods to maximise surgical safety and the fact that a good long term neurological and oncological outcome does not necessarily require a complete resection of the tumour. The authors have addressed comments from the initial reviewers. Although other similar series have been described, these are rare tumours and a relatively large well-described and well-managed series such as this one is still a useful addition to the literature. Within the current paradigms of chemotherapy and targeted therapy for low grade gliomas, their emphasis on surgical safety rather than complete resection is important. This is not always clarified in surgical series.

Kristian Aquilina
London, UK

Authors and Affiliations

Vladimír Beneš 3rd[1] · **Michal Zápotocký[2]** · **Petr Libý[1]** · **Jakub Táborský[1]** · **Jana Blažková Jr[1]** · **Jana Blažková Sr[3]** · **David Sumerauer[2]** · **Adéla Mišove[2]** · **Ivana Perníková[4]** · **Martin Kynčl[5]** · **Lenka Krsková[6]** · **Miroslav Koblížek[6]** · **Josef Zámečník[6]** · **Ondřej Bradáč[1,7]** · **Michal Tichý[1]**

1   Department of Neurosurgery, Second Faculty of Medicine, Charles University and Motol University Hospital, V Úvalu 84, Prague, Czech Republic

2   Department of Paediatric Haematology and Oncology, Second Faculty of Medicine, Charles University and Motol University Hospital, Prague, Czech Republic

3   Department of Anaesthesiology and Intensive Care Medicine, Second Faculty of Medicine, Charles University and Motol University Hospital, Prague, Czech Republic

4   Department of Paediatric Neurology, Second Faculty of Medicine, Charles University and Motol University Hospital, Prague, Czech Republic

5   Department of Radiology, Second Faculty of Medicine, Charles University and Motol University Hospital, Prague, Czech Republic

6   Department of Pathology and Molecular Medicine, Second Faculty of Medicine, Charles University and Motol University Hospital, Prague, Czech Republic

7   Department of Neurosurgery and Neurooncology, First Medical Faculty, Charles University and Military University Hospital, Prague, Czech Republic

Příloha 3

CORRESPONDENCE

Rare *IDH1* variants are common in pediatric hemispheric diffuse astrocytomas and frequently associated with Li-Fraumeni syndrome

David Sumerauer[1,2] · Lenka Krskova[1,3] · Ales Vicha[1,2] · Adela Misove[1,2] · Yasin Mamatjan[4] · Pavla Jencova[1,2] · Marketa Vlckova[5] · Lucie Slamova[2] · Katerina Vanova[1,2] · Petr Liby[6] · Jakub Taborsky[6] · Miroslav Koblizek[3] · Radek Klubal[7] · Martin Kyncl[8] · Gelareh Zadeh[9] · Jan Stary[2] · Josef Zamecnik[1,3] · Vijay Ramaswamy[10,11] · Michal Zapotocky[1,2]

Mutations in isocitrate dehydrogenase 1 (*IDH1*) constitute a frequent somatic driver event in adult low-grade (LGG) and high-grade gliomas (HGG) [1, 3]. In children, *IDH1* mutations are rare and restricted to adolescents with a largely indeterminate incidence and prognosis. Li-Fraumeni syndrome (LFS) is defined as a genetic condition harbouring germline *TP53* mutations, predisposing to multiple early onset cancers including brain tumours [6]. However, our understanding of the genomic landscape of pediatric LFS-associated gliomas is limited by a lack of comprehensive molecular characterization of this group in children [7]. Here, we report *IDH1 R132H* and rare non-R132H *IDH1*

mutations in a cohort of pediatric hemispheric glioma patients who frequently harbour germline *TP53* pathogenic mutations.

To evaluate the incidence of *IDH1* associated hemispheric low-grade gliomas in our population, we screened 76 tumors with available tissue (0–18 years) diagnosed between 2000 and 2018 (Supplementary Table 1, online resource), and performed comprehensive molecular testing using DNA methylation array, somatic and germline DNA panel sequencing, and immunohistochemistry (IHC) for p53 and ATRX (Supplementary Methods, online resource). We identified *IDH1* mutations in 9 of 76 patients (11.8%) with a median age at diagnosis of 12.8 years (range 10.6–17.2) (Treatment and full demographics available in Supplementary Table 2, online resource). Strikingly, only 3/9 (33%) of cases harbored *IDH1 R132H* rather 6/9 (66%) harbored rare *IDH1* variants; specifically, three *IDH1 R132G*, one *R132S*

Vijay Ramaswamy and Michal Zapotocky contributed equally.

Electronic supplementary material The online version of this article (https://doi.org/10.1007/s00401-019-02118-5) contains supplementary material, which is available to authorized users.

✉ Vijay Ramaswamy
vijay.ramaswamy@sickkids.ca

✉ Michal Zapotocky
michal.zapotocky@fnmotol.cz

1   Prague Brain Tumor Research Group, Second Faculty of Medicine, Charles University and University Hospital Motol, Prague, Czech Republic

2   Department of Pediatric Haematology and Oncology, Second Faculty of Medicine, Charles University and University Hospital Motol, V Uvalu 84, Prague 150 06, Czech Republic

3   Department of Pathology and Molecular Medicine, Second Faculty of Medicine, Charles University and University Hospital Motol, Prague, Czech Republic

4   Princess Margaret Cancer Centre and MacFeeters, Hamilton Centre for Neuro-Oncology Research, Toronto, ON, Canada

5   Department of Biology and Medical Genetics, Second Faculty of Medicine, Charles University and University Hospital Motol, Prague, Czech Republic

6   Department of Neurosurgery, Second Faculty of Medicine, Charles University and University Hospital Motol, Prague, Czech Republic

7   Medical Centre Prague, Prague, Czech Republic

8   Department of Radiology, Second Faculty of Medicine, Charles University and University Hospital Motol, Prague, Czech Republic

9   Department of Neurosurgery, Toronto Western Hospital, University of Toronto, Toronto, ON, Canada

10   Division of Pediatric Hematology/Oncology, Programme in Developmental and Stem Cell Biology, Hospital for Sick Children, 555 University Avenue, Toronto, ON M5G1X8, Canada

11   Departments of Medical Biophysics and Paediatrics, University of Toronto, Toronto, ON, Canada

and two *R132C* (Fig. 1a). t-SNE analysis comparing our samples with a previously published reference cohort [2] using 10,000 most differentially methylated probes demonstrated that pediatric IDH1 mutant gliomas cluster within IDH oligodendroglioma and IDH astrocytoma methylation classes and do not represent a distinct group (Fig. 1b). Consistent with our t-SNE analysis, applying the Heidelberg brain tumor classifier resulted in only one sample (*IDH1 R132H*) matching with IDH oligodendroglioma class with 1p/19q codeletion and eight samples were classified as IDH astrocytoma. Within the eight samples which clustered with the IDH astrocytoma class, all harbored *TP53* mutations, and 7/9 had loss of ATRX (Fig. 1a).

Germline pathogenic *TP53* variants were detected in 3/7 patients (PRG 7–9) with available blood samples (43%). Interestingly, two patients with LFS harbored *IDH1 R132G* and one *IDH1 R132C* variant. Additional somatic *TP53* mutations were identified in all cases, ATRX loss was present. 1p/19q loss and *TERT* promoter mutations were not detected. All three patients presented with T2/FLAIR hyperintense, non-enhancing subcortical lesions of the frontal lobe. Two patients (PRG7 and PRG8) had frontal lesion detectable on MRI seven years prior the surgery which was performed based on the tumour growth (Supplementary Fig. 1, online resource).

Five-year progression-free survival in IDH mutant glioma was 0.33 (95% CI 0.13–0.84) and two patients died of disease (Supplementary Fig. 2, online resource). PRG2 experienced multiple progressions and development into MRI appearance of gliomatosis cerebri over a 9-year interval. PRG8 died of metastatic renal cell carcinoma and was disease free in regards of her IDH astrocytoma.

Herein we report that non-R132H somatic events in *IDH1* are common genetic drivers of pediatric hemispheric diffuse astrocytomas and are frequently associated with LFS. Current methods of detecting *IDH1* mutational status rely primarily on immunohistochemistry or droplet digital PCR which is specific to the detection of the *IDH1 R132H* mutation. Indeed, our findings suggest that *IDH1* mutations will be missed in the majority of pediatric IDH astrocytoma, and evaluation of rare *IDH1* variants is crucial in this group of patients. This might be applicable for pediatric IDH HGG which seems to represent less than 10% of hemispheric HGG based on previous reports [5] and our unpublished observations of *IDH1/2* mutations in 6.6% of cases.

Recently, Orr et al. reviewed LFS-associated brain tumours describing adults at risk of developing diffuse astrocytomas harbouring *IDH1 R132C* mutation [6, 7]. Our data demonstrate that children with LFS may develop not only *IDH1 R132C* but also *IDH1 R132G* associated with ATRX loss, but without *TERT* promoter mutation. Moreover, there are previous anecdotal reports suggesting that *IDH1* mutations exist in CMMRD [4]. Our results support a model where all children with *IDH1* mutant gliomas should be screened for cancer predisposition syndromes (CPS), and gliomas in patients with CPS should be screened for *IDH1* mutations including non-R132H variants. Moreover, published evidence indicates that LFS is probably rare in *IDH1*
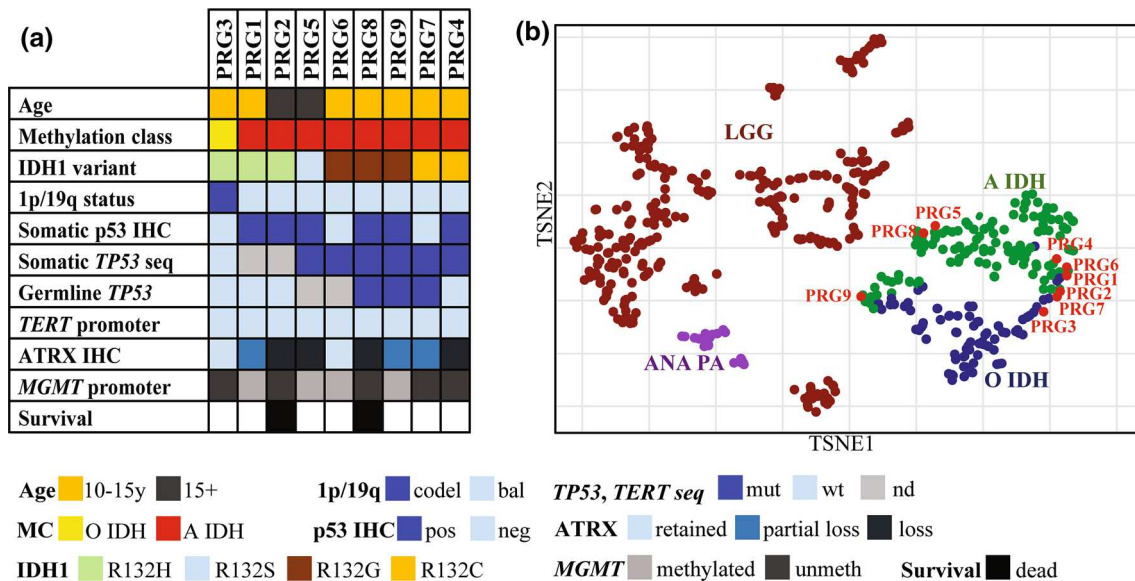

Fig. 1 a Oncoplot demonstrating genetic and epigenetic features of pediatric IDH gliomas. **b** t-SNE plot displays LGG tumour types from 2801 reference samples (https://www.ncbi.nlm.nih.gov/geo, GSE90496) and nine Prague samples demonstrating clustering within methylation classes of IDH oligodendroglioma and IDH astrocytoma.

A IDH IDH astrocytoma class, *codel* codeletion, *IHC* immunohistochemistry, *MC* methylation class, *mut* mutant, *nd* not done, *neg* negative, *O IDH* IDH oligodendroglioma class, *pos* positive, *unmeth* unmethylated, *wt* wild-type

wild-type LGG. For example, none of the 40 LGG (within large cohort accounting for over 1000 cancer patients) harboured pathogenic *TP53* mutations [8].

Our findings using genome wide DNA methylation profiling indicate that pediatric IDH gliomas do not differ epigenetically from classical adult onset IDH related gliomas, where the natural history would suggest eventual malignant progression. This is consistent with previous reports using similar analytic approaches demonstrating childhood IDH HGG being biologically similar to their adult counterparts [5]. This could have therapeutic implications with respect to considering more aggressive measures, such as complete surgical resection with wide margins and/or initiation of temozolomide to potentially avoid future malignant transformation. The emergence of non-invasive methods of detecting *IDH1* mutations, specifically the identification of the oncometabolite alpha-ketoglutarate using advanced magnetic resonance spectroscopy can allow the identification of small pre-malignant lesions during routine surveillance in patients with CPS.

Our report adds to the emerging data that driver events in pediatric CPS converge on known hotspot genes such as *IDH1*. Direct sequencing of *IDH1* should be an essential part of the workup for any LFS-associated glioma, and conversely, the identification of *IDH1* mutations in diffuse gliomas of childhood and adolescence warrant an extensive workup for CPS.

References

1. Cancer Genome Atlas Research N, Brat DJ, Verhaak RG, Aldape KD, Yung WK, Salama SR et al (2015) Comprehensive, integrative genomic analysis of diffuse lower-grade gliomas. N Engl J Med 372:2481–2498. https://doi.org/10.1056/NEJMoa1402121
2. Capper D, Jones DTW, Sill M, Hovestadt V, Schrimpf D, Sturm D et al (2018) DNA methylation-based classification of central nervous system tumours. Nature 555:469–474. https://doi.org/10.1038/nature26000
3. Eckel-Passow JE, Lachance DH, Molinaro AM, Walsh KM, Decker PA, Sicotte H et al (2015) Glioma groups based on 1p/19q, IDH, and TERT promoter mutations in tumors. N Engl J Med 372:2499–2508. https://doi.org/10.1056/NEJMoa1407279
4. Galuppini F, Opocher E, Tabori U, Mammi I, Edwards M, Campbell B et al (2018) Concomitant IDH wild-type glioblastoma and IDH1-mutant anaplastic astrocytoma in a patient with constitutional mismatch repair deficiency syndrome. Neuropathol Appl Neurobiol 44:233–239. https://doi.org/10.1111/nan.12450
5. Mackay A, Burford A, Molinari V, Jones DTW, Izquierdo E, Brouwer-Visser J et al (2018) Molecular, pathological, radiological, and immune profiling of non-brainstem pediatric high-grade glioma from the HERBY phase II randomized trial. Cancer Cell 33(5):829–842.e5. https://doi.org/10.1016/j.ccell.2018.04.004
6. Orr BA, Clay MR, Pinto EM, Kesserwan C (2019) An update on the central nervous system manifestations of Li-Fraumeni syndrome. Acta Neuropathol Rev. https://doi.org/10.1007/s00401-019-02055-3. **(Epub ahead of print)**
7. Watanabe T, Vital A, Nobusawa S, Kleihues P, Ohgaki H (2009) Selective acquisition of IDH1 R132C mutations in astrocytomas associated with Li-Fraumeni syndrome. Acta Neuropathol 117:653–656. https://doi.org/10.1007/s00401-009-0528-x
8. Zhang J, Walsh MF, Wu G, Edmonson MN, Gruber TA, Easton J et al (2015) Germline mutations in predisposition genes in pediatric cancer. N Engl J Med 373(24):2336–2346. https://doi.org/10.1056/NEJMoa1508054
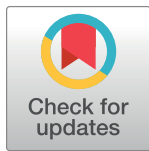
Příloha 4

PLOS ONE

Older age is a protective factor for academic achievements irrespective of treatment modalities for posterior fossa brain tumours in children

Jarmila Kruseova[1]*, Anna Sarah Kovacova[2], Michal Zapotocky[1], David Sumerauer[1], Ivana Pernikova[3], Darja Starkova[2], Adela Misove[1], Andrea Zichova[1], Vaclav Capek[4], Thorsten Langer[5], Antoinette am Zehnhoff-Dinnesen[6], Tomas Eckschlager[1], Martin Kyncl[2]

1 Department of Paediatric Haematology and Oncology, Charles University, 2nd Faculty of Medicine and University Hospital Motol, Prague, Czech Republic, 2 Department of Radiology, Charles University, 2nd Faculty of Medicine and University Hospital Motol, Prague, Czech Republic, 3 Department of Paediatric Neurology, Charles University, 2nd Faculty of Medicine and University Hospital Motol, Prague, Czech Republic, 4 Bioinformatics Centre, Charles University, 2nd Faculty of Medicine and University Hospital Motol, Prague, Czech Republic, 5 Pediatric Oncology and Hematology, University Hospital for Children and Adolescents, Lübeck, Germany, 6 Department of Phoniatrics and Pedaudiology, University Hospital Münster, Münster, Germany

* jarmila.kruseova@fnmotol.cz

Abstract

The treatment of children with posterior fossa brain tumours (PFBT) impacts their long term functional and imaging outcomes. This study aimed to evaluate academic achievement correlated with long-term sequelae after different PFBT treatment modalities. The study cohort consisted of 110 survivors (median age at diagnosis 10.1 years and median time of follow up 13.2 years) who completed hearing questionnaires, neurological assessment and MRI of the brain $\geq$5 years after the end of treatment. There were three treatment groups. A cisplatin group which underwent cisplatin chemotherapy, radiotherapy and surgery (medulloblastoma N = 40), a radiotherapy group which underwent radiotherapy and surgery (astrocytoma/ependymoma N = 30), and a surgery group (astrocytoma N = 40). Academic achievement was correlated to the age at diagnosis, ototoxicity, Karnofsky score (KS), and MRI findings (Fazekas Score (FS)- treatment related parenchymal changes). For a modelled age at diagnosis of five years, the cisplatin group had lower academic achievements compared to the radiotherapy ($p = 0.028$) and surgery ($p = 0.014$) groups. Academic achievements evaluated at a modelled age of 10 years at diagnosis did not significantly differ among the treatment groups. The cisplatin group exhibited a higher occurrence of ototoxicity than the radiotherapy ($p < 0.019$) and surgery groups ($p < 0.001$); however, there was no correlation between ototoxicity and academic achievements ($p = 0.722$) in older age at diagnosis. The radiotherapy group exhibited lower KS than the surgery group ($p < 0.001$). KS significantly influenced academic achievements in all groups ($p < 0.000$). The cisplatin group exhibited higher FS than the surgery group ($p < 0.001$) while FS did not correlate with

---

academic achievement (p = 0.399). Older age is a protective factor for academic achievements irrespective of a treatment modality.

Introduction

With the advent of modern treatment approaches, more than 70% of children diagnosed with primary Central Nervous System (CNS) cancers are surviving longer than five years after the end of treatment [1–3]. One of the factors contributing to this increased number of survivors is the result of intensified therapies, many of which employ cisplatin-based regimens and radiotherapy. However, long-term toxicity remains a major problem for these survivors which significantly affects their quality of life [1–3]. Sensorineural hearing loss (SNHL) is an important consequence of cisplatin chemotherapy [4–6]. Cranial radiotherapy is less ototoxic than cisplatin-based treatment but is still associated with a high risk of SNHL which is even more pronounced when combined with cisplatin [1, 5]. Though studies confirmed a correlation between hearing loss and academic achievements in patients younger than 5 years at diagnosis [1,5], longitudinal reports of SNHL in childhood cancer survivors are limited [4, 6]. Chemo-irradiation and tumour-related effects lead to other long-term consequences, including neuro-cognitive deficits such as learning and memory deficits [1, 4]. This can negatively influence academic achievements [3, 4, 7, 8]. Posterior fossa brain tumour (PFBT) survivors can be affected by all of the late neurological effects mentioned above [7, 9]. However, the relative role of different neurotoxic effects of PFBT treatment modalities are poorly understood [7]. This central neurotoxicity may manifest as radiological imaging abnormalities [7–10]. The most studied are these two changes the alteration of white matter (WM) and cerebral atrophy (CA) which are detectable by MRI [7–10]. These MRI findings develop more frequently after chemo-irradiation compared to radiotherapy alone and are associated with poor cognitive performance and IQ scores [9, 10]. To our knowledge, there has been no published study of PFBT survivors and correlations between academic achievement, MRI findings and late effect sequelae with a median follow-up longer than 12 years.

In the current study we took advantage of a long follow-up of our PFBT survivors to clarify the role of older age at diagnosis in cases of different treatment modalities. Firstly, we aimed to evaluate academic achievement correlated with age at diagnosis and long-term sequelae after PFBT, using different treatment modalities. Secondly, we correlated the presence of these late effects among PFBT survivors and MRI brain imaging findings.

Material and methods

Patient cohort

We conducted a retrospective study of long-term survivors treated for PFBT at the Department of Paediatric Haematology and Oncology, University Hospital Motol, Prague, Czech Republic, between the years 1980–2012. Within this period, the total number of CNS tumour survivors were 634. Survivors treated with methotrexate (neurotoxicity risk) (N = 31), who had genetic syndromes (N = 98) or developed relapses (N = 52) or subsequent neoplasms (N 32) were excluded. We excluded patients who reported hearing impairments in their family history, including siblings (N = 3). From the remaining cohort 110 of whom were included subject to the application of the following inclusion criteria: 1) PFBT survivors; 2) completed hearing questionnaire as part of the PanCareLIFE* ototoxicity study (2014–2017); 3)

neurological assessment; and 4) MRI of the brain (2014–2017). All correlations were conducted using data collected at least five years after the end of treatment.

We evaluated academic achievement in PFBT survivors with regard to age at diagnosis and other long-term consequences, such as ototoxicity, Karnofsky Score (KS), and MRI findings. PFBT survivors were divided into three groups according to the therapy they had received: the cisplatin group received all treatment modalities [cisplatin-based regimens, radiotherapy, and surgery] (N = 40); the radiotherapy group consisted of patients who had undergone radiotherapy and surgery (N = 30); and the surgery group comprised patients who had undergone a surgical procedure only (N = 40). The observed groups did not differ statistically in age at diagnosis, sex, and age during evaluation. The presence of decompensated hydrocephalus at diagnosis with ventriculoperitoneal (VP) shunt placement during study evaluation and follow-up was higher in the radiotherapy group. The patients' characteristics are summarized in Table 1.

Academic achievements

We correlated academic achievements for patients > 22 years (N = 85) (Scale: 0 psychomotor retardation, 1 primary school, 2 secondary school without graduation, 3 high school, 4 university).

Hearing impairment evaluation

As part of the PanCareLIFE* study (2014–2017), all participants filled out self-reported questionnaires regarding hearing impairment, hearing aids, and tinnitus. For statistical evaluation, we used the following scale: 0 = no hearing impairment; 1 = self-reported hearing problems including tinnitus without the need of a hearing aid; 2 = hearing aid; and 3 = deafness. The definition of severe ototoxicity in present study was grade 2 and grade 3 together. All patients had normal hearing before oncology treatment.

Neurological outcomes

For neurology assessment we used standard KS evaluation [11] and incidence of epilepsy based on the need for current medication. The neurological examination included evaluation of: 1) motoric functions (muscle tone, tendon reflexes, cerebellar functions, fine hand motor skills; 2) neurocognitive functions (attention, memory, processing speed); 3) practical skills and 4) mental functions (conclusions of school reports, the need for certain adjustments, individual programs, emotional and adjustment problems, working experiences, questions about other activities and hobbies). KS definition: 100 = normal, no complaints; 90 = able to carry on normal activities, with minor signs or symptoms of disease; 80 = normal activity with effort, with some signs and symptoms of disease; 70 = cares for self but unable to carry on normal activity or to perform work; 60 = requires occasional assistance but is able to take care of most personal needs; 50 = requires frequent assistance and medical care; 40 = disabled, requires special care and assistance; and 30 = severely disabled. All of our study's long-term survivors were seen by one senior neurologist specializing in cancer late effects.

Imaging outcome measures

MRI scans were retrospectively reviewed for the following changes: brain atrophy, surgery-related focal abnormalities, and chemo/radiotherapy treatment-related focal or generalized parenchymal changes. Brain atrophy was assessed using a subjective visual grading system categorized as absent or present. Postoperative parenchymal changes were recorded as appropriate or extended by subjective visual grading. As part of the categorization of focal brain

Table 1. Patients characteristics.

Characteristics	Cisplatin group	Radiotherapy group	Surgery group	Significance among groups
Total number of patiens	N 40	N 30	N 40	
Female/ Male	**17(43%) / 23 (57%)**	**18 (60%) / 12 (40%)**	**18(45%)/22 (55%)**	**p = 0.308**
Histopathology	Medulloblastoma	Ependymoma gr.III 9 (30%)	Astrocytoma gr. I 26 (65%)	--
	Classic 15(38%)			
	Desmoplastic 6(15%)	Astrocytoma gr. II/III 17 (57%)	Astrocytoma gr.II 14 (35%)	
	Anaplastic 5(12%)			
	Unclassified 14(35%)	Astrocytom gr. I 4 (13%)		
Hydrocephalus at dg. [1] + VP shunt [2] number of patients.	N7 (17%)	N 13 (43%)	N 10 (25%)	p = 0.052
Median ± IQR age at dg. [2] (years)	9.5 (6.7–11.9)	12.4 (5.8–17.7)	11.1 (5.6–14.3)	p = 0.366
Median ± IQR FUP[3] since dg. [1] (years)	12.4 (8.6–15.5)	14.7 (11.8–17.5)	11.9 (9.2–14.6)	P = 0.050*
Median ± IQR age at the time of investigation (years)	22.3 (19.5–27.1)	24.5 (21.2–32.2)	22.5(18.0–25.9)	p = 0.080
Treatment period	1990–1999 N7 (18%)	1991–1999 N9 (30%)	1992–1999 N6(15%)	--
Years/number of patients	2000–2004 N17 (42%)	2000–2004 N15 (50%)	2000–2004 N14(35%)	
	2005–2011 N16 (40%)	2005–2011 N 6 (20%)	2005–2012 N20(50%)	
Subtotal/Complete surgery	13 (33%)/ 27(67%)	18 (60%)/ 12 (40%)	13(33%)/27(67%)	--
Radiotherapy			--	--
Posterior fossa dose	55.8 Gy (50.0–59.8)	54.6Gy (50–59.8)		
Craniospinal dose	25.4 Gy (24.9–30.6)	N2 30 Gy		
Cisplatin median dose	470.5 mg/m^2	--	--	--
CCGA9961[4]				
Standard risk patients N = 25	544 mg/m^2 [6]			
High risk patients N = 11	300 mg/m^2 [7]			
7 in one protocol[5] N = 4	480 mg/m^2 [8]			

* statistically signifiant, IQR: interquartile range, [1] dg.–diagnosis, [2] hydrocephalus and VP shunt–initially decompensated hydrocephalus and than ventriculoperitoneal shunt placement, [3] FUP- follow up.

[4–5] Medulloblastoma treatment protocols with cisplatin: CCGA9961—Children's Cancer Group/Pediatric Oncology Group study number A 9961 and "7 in one protocol". Study patients received following cumulative dose of cytostatics according these protocols.

CDDP—cisplatin, VCR—vincristine, CCNU—lomustine, CYC–cyclophosphamide.

[6]CDDP 544 mg/m^2–8 courses 68 mg/m^2, concomitant cytostatic: VCR 48 mg/m^2, CCNU 600 mg/m^2.

[7] CDDP 300 mg/m^2–4 courses 75 mg/m^2, concomitant cytostatics: VCR 12 mg/m^2, CYC 16000 mg/m^2.

[8] CDDP 480 mg/m^2–6 courses 80 mg/m^2, concomitant cytostatics: VCR 12 mg/m^2, CYC 2400 mg/m^2, CCNU 600 mg/m^2, procarbazine 600 mg/m^2, cytarabine 2400 mg/m^2, hydroxyurea 12 000 mg/m^2.

https://doi.org/10.1371/journal.pone.0243998.t001

lesions, we used the Fazekas score (FS) to detect T2 / FLAIR hyperintense foci. FS was categorized according to the treatment-related parenchymal changes (0 none/single lesion; 1 multiple punctate; 2 beginning confluence of lesions; 3 large confluent lesions). When employing FS, we used the following methodologies [12, 13]. The MRI studies included FLAIR sequences (slice thickness 4–5 mm). Each MR image was evaluated independently by two readers in consensus: a senior consultant radiologist with expertise in paediatric radiology and a resident radiologist with 4 years of experience in paediatric imaging in the field. The radiologists did not have information about detailed oncology treatment and subsequent complications. MRI was conducted on 1.5 Tesla scanners (Achieva and Intera, Philips, The Netherlands, Avanto, Siemens, Germany).

Statistical analysis

Differences in baseline Patients´ characteristics among the studied groups of patients, see Table 1, were studied using chi^2 test, parametric ANOVA and the Kruskal-Wallis test. Risks of ototoxicity, epilepsy, tinnitus, atrophy, post-operative changes, and FS were modelled by logistic regression. Influence of the treatment and the age at diagnosis on the highest education level was examined using a multivariable ordinal logistic regression with an interaction between the treatment and the age. In this model possible confounders (gender, FUP, and hydrocephalus with VP shunt placement) were also considered. Effect of the treatment on KS was modelled by linear regression with a dependent variable being transformed using a Box-Cox transformation. All p values are reported as two-sided, using 0.05 as the level of significance. Analyses were conducted using an R statistical package, version 3.4.2, R Core Team (2017).

Ethics statement

Written informed consent for using their ototoxicity and education questionnaires was obtained from all study participants > 18 years and for participants < 18 years was obtained from parents/legal guardians for these patients. Those results were part of PanCareLife Studies in Fertility and Otoxicity to Improve Quality of Life after Cancer during Childhood, Adolescence and Young Adulthood—we received ethical favorable opinion–Ethics Committee for Multi-Centric Clinical Trials of the University Hospital Motol 1.4.2014 –Reference No.: EK-478/14. Neurology assessment and brain MRI were part of standard routine follow up care–all included patients provided informed written consent to have data from their medical records used in research with strictly anonymous data. Ethical approval of this part of present study was waived by the local Ethics Committee of Motol University Hospital in view of the retrospective nature of the study and all the procedures being performed were part of the routine care. We retrospectively evaluated medical records 4.2014–12.2017.

Results

Age at diagnosis strongly influences academic achievements in PFBT survivors

The modelled age of 5 years at diagnosis for the cisplatin group exhibited significantly decreased academic achievements compared to the radiotherapy and surgery groups. In contrast, academic achievements evaluated at a modelled age of 10 years at diagnosis did not significantly differ among the groups. We confirmed a negative young age effect at diagnosis on further academic achievements only in the cisplatin group (p = 0.003). From 85 patients > 22 years six patients completed university studies (15%) in the cisplatin group, compared to 9 patients (30%) in the radiotherapy group and 9 patients (23%) in the surgery group. Statistical correlations of academic achievements among the observed groups and the modelled age at diagnosis are shown in Table 2.

Significant risk of hearing impairment after radiation and cisplatin-based therapy

The overall incidence of self-reported hearing problems in the observed groups was 25%. The cisplatin group had 21 patients (53%) who reported hearing impairment, including eight patients (21%) with severe ototoxicity (hearing aid in seven patients and deafness in one patient). The radiotherapy group had six patients (20%) with four suffering from severe ototoxicity (13%) (hearing aid in three patients and deafness in one patient). In the surgery group, only one patient had a mild hearing impairment. Statistical correlations of hearing

Table 2. Academic achievements–multivariable model.

Parameter	Estimate	SE	z-value	p-value
A. Full model containing all confounders considered				
surgery group[1]	4.6495	1.0570	4.3986	0.0000
radiotherapy group[2]	4.4431	1.1959	3.7152	0.0002
Age	0.3892	0.0838	4.6441	0.0000
FUP	0.1011	0.0374	2.7010	0.0069
Hydrocephalus at dg.+ VP shunt	0.8430	0.4319	1.9518	0.0510
Gender	0.1066	0.3750	0.2844	0.7761
surgery group:age	-0.3675	0.0997	-3.6842	0.0002
radiotherapy group:age	-0.4311	0.1151	-3.7451	0.0002
B. Reduced model containing only statistically significant parameters				
surgery group	4.2479	1.0347	4.1053	0.0000
radiotherapy group	3.9745	1.1584	3.4310	0.0006
Age	0.3800	0.0826	4.6011	0.0000
FUP	0.1018	0.0365	2.7880	0.0053
surgery group:age	-0.3360	0.0977	-3.4381	0.0006
radiotherapy group:age	-0.4079	0.1125	-3.6248	0.0003
C. Post-hoc tests of the effect of age in treatment groups				
cisplatin group	0.380	0.083	4.601	0.000
surgery group	0.044	0.059	0.744	0.839
radiotherapy group	-0.028	0.074	-0.379	0.974
D. Post-hoc tests of the difference between treatment groups in modelled age of 5 years				
cisplatin vs. surgery group	2.568	0.620	4.142	0.000
cisplatin vs. radiotherapy group	1.935	0.687	2.817	0.013
surgery vs. radiotherapy group	-0.633	0.656	-0.965	0.598
E. Post-hoc tests of the difference between treatment groups in modelled age of 10 years				
cisplatin vs. surgery group	0.888	0.419	2.119	0.086
cisplatin vs. radiotherapy group	-0.105	0.485	-0.216	0.975
surgery vs. radiotherapy group	-0.992	0.488	-2.032	0.104

[1]surgery group: age–interaction between age and the effect of surgery with respect to cisplatin.

[2]radiotherapy group: age–interaction between age and the effect of radiotherapy with respect to cisplatin.

https://doi.org/10.1371/journal.pone.0243998.t002

impairments among the observed groups are provided in Table 3. We did not confirm any correlation between hearing impairment and academic achievements (p = 0.723).

Performance status scores depend on treatment modalities and the presence of hydrocephalus

KS scores of 90–100 were observed in 17 patients (43%) in the cisplatin group, in 11 patients (36%) in the radiotherapy group, and in 33 patients (83%) in the surgery group. For KS

Table 3. Hearing impairment.

Risk factors	Estimate	SE	z- value	p-value
Hearing impairment				
Cisplatin group vs. surgery gr.	3.764	1.061	3.547	0.001**
Cisplatin group vs. radiotherapy gr.	1.486	0.556	2.676	0.019*
Surgery gr. vs. radiotherapy gr.	-2.277	1.111	-2.050	0.094

https://doi.org/10.1371/journal.pone.0243998.t003

distribution among the observed groups see Fig 1A. KS was significantly lower in the cisplatin group vs. surgery group (p<0.010) as well as in the radiotherapy group vs. surgery group (p<0.001), but no significant difference was observed between the cisplatin and radiotherapy groups (p = 0.628). We confirmed correlation between decreased KS and the presence of decompensated hydrocephalus at dg. and VP shunt placement in all observed groups (p = 0.022) Fig 1B. There was no correlation between academic achievement and the presence of hydrocephalus at diagnosis (p = 0.110). Highly significant correlation between lower KS and worse academic achievement (p<0.000) was confirmed in all groups Fig 1C.

(0 – psychomotor retardation; 1 – primary school; 2 – secondary school without graduation; 3 – high school; 4 – university)
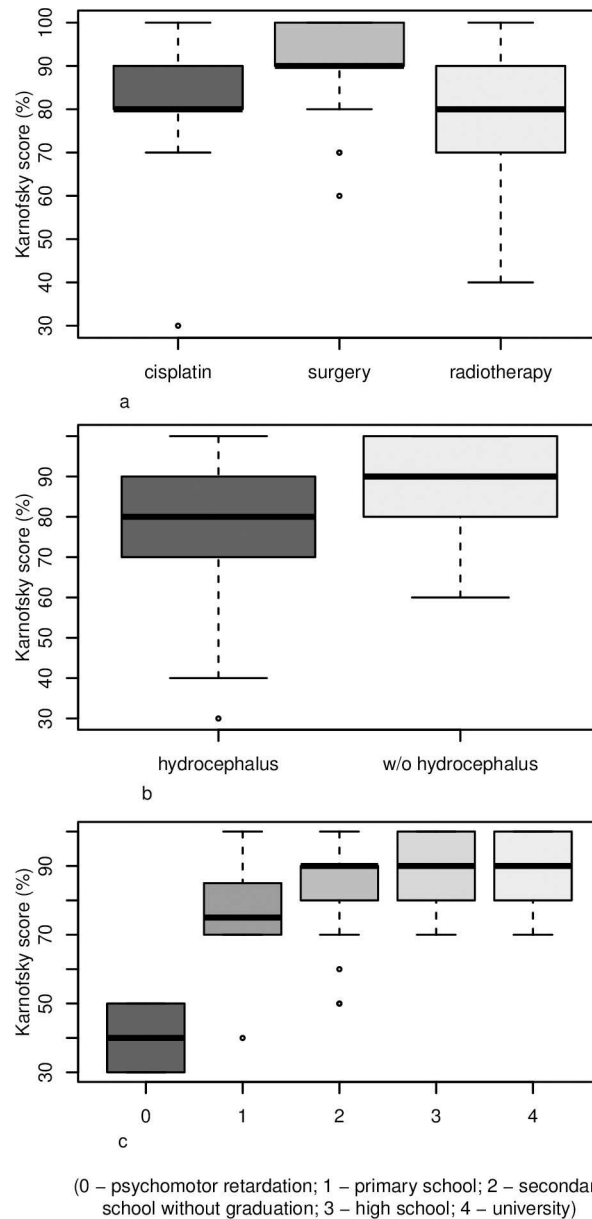
Fig 1. A. Comparison of the treatment groups and KS score distribution. **B.** Comparison of hydrocephalus diagnosed at cancer diagnosis and its effect on KS distribution. **C.** Comparison of KS score distribution and its effect on academic achievements.

https://doi.org/10.1371/journal.pone.0243998.g001

Treatment-related MRI changes correlate with performance status

Brain atrophy was observed in 11 patients (27%) in the cisplatin group, in four patients (13%) in the radiotherapy group, and in eight patients (20%) in the surgery group. We did not observe any group effect on brain atrophy development (p = 0.488). Extensive postoperative changes were seen in six patients (15%) in the cisplatin group, in 14 patients (47%) in the radiotherapy group, and in seven patients (18%) in the surgery group Fig 2A). There were differences between the radiotherapy group and the cisplatin group (p<0.014) and the surgery group (p<0.017). We did not confirm correlation between the extent of postoperative changes and academic achievements (p = 0.35). White matter changes characterized by FS >1 were seen in 13 patients (33%) in the cisplatin group and in six patients (20%) in the radiotherapy group (p = 0.189). The surgery group had no WM changes Fig 2B. Analysis confirmed that higher FS correlated with worse KS in all groups (p = 0.033). Furthermore, young age at diagnosis correlated with more extensive white matter changes and higher FS was observed (p<0.009). Correlation of FS and academic achievement was on the border of statistical significance in the cisplatin group (p = 0.072). When evaluating all groups together, there was no correlation between FS and academic achievements (p = 0.399).

Discussion

One of the key questions for cancer survivors who are cured is "what my quality of my future life will be". The level of academic achievement is of great importance for many survivors. Our study provides and explains which treatment modalities and late sequelae affect academic
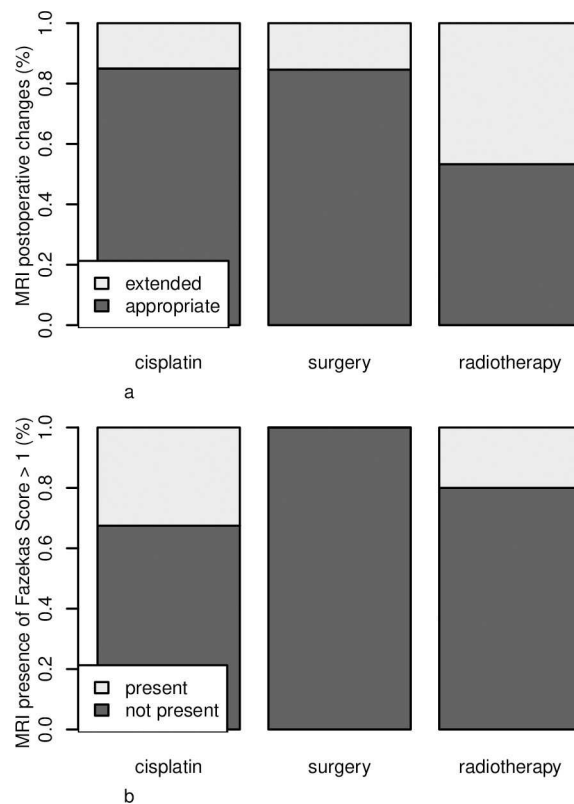

Fig 2. A. Comparison of the treatment groups and MRI presence of postoperative changes. **B.** Comparison of the treatment groups and MRI presence of FS>1.

https://doi.org/10.1371/journal.pone.0243998.g002

achievements. Compared to previously published studies [4, 5], our analysis was based on different treatment modalities in long-term PFBT survivors who were older at diagnosis.

The overall incidence of self-reported hearing problems in our groups was 25%. These findings are similar to previous Children Cancer Group (CCG) study where the prevalence of self-reported hearing loss was 20% [14]. Severe ototoxicity was present in 35% of patients in the cisplatin group compared to 20% of patients in the radiotherapy group, what is in accordance with previous ototoxicity studies [1, 15, 16]. We did not identify correlation between self-reported hearing impairments and academic achievements, which is in contrast to Brinkman et al [1] who observed that hearing loss was perceived to have a negative impact on education. In their study, the prevalence of serious ototoxicity was 36%. Although our cisplatin group had the same prevalence of serious hearing loss (35%) we did not confirm their results. A possible explanation follows from the fact that our study included children who were older at the time of diagnosis. Previous studies reported the effects of hearing loss with regards to academic achievement but all in patients younger than 5 years at diagnosis [1, 5, 16].

We observed a negative effect of young age at diagnosis on further academic achievements only in the cisplatin group. This finding is in conformity with a theory regarding CNS survivors having a reduced ability to learn new information with a significant effect of age at diagnosis [2]. We confirmed that older age at diagnosis did not affect academic achievements among all of the observed groups despite the treatment modality applied. Therefore, this result and our previous findings further support our hypothesis of the "protective effect of age".

Neurotoxicity due to specific chemotherapeutic agents has been described for methotrexate, alkylating agents (i.e., cisplatin, ifosfamide, cyclophosphamide) and others such as carmustine, cytosine arabinoside, and vincristine [8, 9, 17–19]. In order to better understand the impact of cisplatin on academic achievements, we excluded all regimens comprising methotrexate which quite often results in learning disabilities [8, 17, 19]. Our patients were treated with chemotherapeutic regimens that included some of the cytostatics mentioned above; therefore, there might be an additive effect of other cytostatics on cisplatin itself. We found the highest difference in academic achievements in younger children between medulloblastoma and pilocytic astrocytoma, which is in line with the study of Duffner et al [17] who found that children with medulloblastoma had significantly worse IQ than children with cerebellar astrocytoma.

PFBT survivors can develop a range of persistent late effects in neuro-cognitive, sensation, and functional abilities [3, 9–11, 20–22]. We decided to use KS because it is the most complex available tool for neurology assessment. There was a strong correlation between KS and academic achievements irrespective of treatment modalities. We did not observe additional negative effects of cisplatin treatment on KS. No worsening of KS was present even in case of whole craniospinal irradiation in the cisplatin group compared to focal PFBT irradiation in the radiotherapy group. In concordance with the work of Rueckriegel et al. [7], our study revealed that hydrocephalus at diagnosis also contributed to a decrease in KS. In contrast to a study by Lassaletta et al. [22], in which children with PFBT and the presence of hydrocephalus had significantly worse academic outcomes, we did not observe this correlation. Late effects tend to be aggravated with time [3–5, 23]; consequently, we suppose that another factor contributing to the lowest KS in the radiotherapy group could be the longer follow-up time in this group.

Conventional magnetic resonance imaging (MRI) can identify some long-term changes of the central nervous tissue, such as morphologic local damage, brain atrophy, and alterations of WM [7, 9, 12, 24–28]. The highest number of WM changes were seen in the cisplatin group, which is consistent with previous publications where medulloblastoma treatment exhibited a high risk of WM damage [7, 9, 21]. The differences in FS between the cisplatin and radiotherapy groups did not reach statistical significance, but we supposed that there could be some additive effects of cisplatin-based regimens on WM changes. Unlike previous studies in which

MRI abnormal WM volume correlated with increasing deficits in intelligence and academic performance [9, 24], we could not adamantly support this finding in our study cohort. We only confirmed correlation between FS and KS in the cisplatin and radiotherapy groups. It was only FS that showed the group effect of age at diagnosis. Younger patients at the beginning of treatment had higher FS [9]. Since we included older patients at diagnosis, we assumed that FS was not so frequent in our study cohort and we did not observe negative influence of WM changes on academic achievement.

The limitations of our study are the longer follow-up and the higher presence of hydrocephalus at diagnosis in the radiotherapy only patients, which could influence the evaluation of the additional effects of the cisplatin treatment. Another limit of this study aimed at assessing educational attainment is that the presence of various other chronic consequences from previous cancer treatment (endocrine, renal, cardiac, sleeping disorders, chronic fatigue syndrome etc.) and survivors psychological well-being may influence academic achievement. The family, social conditions, and motivation also play an important role. These factors were not in current study evaluated.

Conclusions

Our long-term data were able to compare different late sequelae in patients treated for PFBT. We can confirm that the group of younger children who were treated with surgery, craniospinal radiation, and cisplatin-based regimen were the most vulnerable one, having the highest incidence of hearing impairments and the lowest academic achievement. Treatment modalities in all groups did not differ in their effects on academic achievement among older children. We did not observe, except KS, any impact of ototoxicity and MRI findings after different PFBT treatments on academic achievements in patients who were older at diagnosis.

Supporting information

S1 Dataset. List of patients data and outcomes.
(XLSX)

Author Contributions

Conceptualization: Jarmila Kruseova, Martin Kyncl.

Data curation: Anna Sarah Kovacova, David Sumerauer, Ivana Pernikova, Darja Starkova, Adela Misove, Andrea Zichova.

Formal analysis: Vaclav Capek.

Funding acquisition: Jarmila Kruseova.

Investigation: Jarmila Kruseova, Martin Kyncl.

Methodology: Michal Zapotocky, David Sumerauer, Tomas Eckschlager.

Software: Vaclav Capek.

Supervision: Jarmila Kruseova, Thorsten Langer, Antoinette am Zehnhoff-Dinnesen, Martin Kyncl.

Validation: Darja Starkova.

Writing – original draft: Jarmila Kruseova, Martin Kyncl.

Writing – review & editing: Anna Sarah Kovacova, Michal Zapotocky, David Sumerauer, Ivana Pernikova, Darja Starkova, Adela Misove, Andrea Zichova, Vaclav Capek, Thorsten Langer, Antoinette am Zehnhoff-Dinnesen, Tomas Eckschlager.

References

1. Brinkman TM, Bass JK, Li Z, Ness KK, Gajjar A, Pappo AS, et al. Treatment-induced hearing loss and adult social outcomes in survivors of childhood CNS and non-CNS solid tumors: Results from the St. Jude Lifetime Cohort Study. Cancer. 2015; 121: 4053–4061. https://doi.org/10.1002/cncr.29604 PMID: 26287566

2. Rowe LS, Krauze AV, Ning H, Camphausen KA, Kaushal A. Optimizing the benefit of CNS radiation therapy in the pediatric population-PART 1: understanding and managing acute and late toxicities. Oncology. 2017; 31: 182–188. PMID: 28299754

3. Armstrong GT, Conklin HM, Huang S, Srivastava D, Sanford R, Ellison DW, et al. Survival and long-term health and cognitive outcomes after low-grade glioma. Neuro Oncol. 2011; 13:223–234. https://doi.org/10.1093/neuonc/noq178 PMID: 21177781

4. Orgel E, O'Neil SH, Kayser K, Orgel E, O'Neil SH, Kayser K, et al. Effect of Sensorineural Hearing Loss on Neurocognitive Functioning in Pediatric Brain Tumor Survivors. Pediatr Blood Cancer. 2016; 63:527–534. https://doi.org/10.1002/pbc.25804 PMID: 26529035

5. Bass JK, Hua CH, Huang J, Onar-Thomas A, Ness KK, et al. Hearing Loss in Patients Who Received Cranial Radiation Therapy for Childhood Cancer. J Clin Oncol. 2016; 34:1248–1255. https://doi.org/10.1200/JCO.2015.63.6738 PMID: 26811531

6. Scobioala S, Parfitt R, Matulat P, Ebrahimi F, Wolters H, Zehnhoff-Dinnesen A, et al. Impact of radiation technique, radiation fraction dose, and total cisplatin dose on hearing: retrospective analysis of 29 medulloblastoma patients. Strahlentherapie und Onkologie. 2017; 193: 910–920. https://doi.org/10.1007/s00066-017-1205-y PMID: 28887665

7. Rueckriegel SM, Driever PH, Bruhn H. Supratentorial neurometabolic alterations in pediatric survivors of posterior fossa tumors. Int J Radiat Oncol Biol Phys. 2012; 82:1135–1141. https://doi.org/10.1016/j.ijrobp.2011.04.017 PMID: 21658852

8. Sleurs C, Deprez S, Emsell L, Lemiere J, Yuttebroeck A. Chemotherapy-induced neurotoxicity in pediatric solid non-CNS tumor patients: an update on current state of research and recommended future directions. Crit Rev Oncol Hematol. 2016; 103:37–48. https://doi.org/10.1016/j.critrevonc.2016.05.001 PMID: 27233118

9. Khong PL, Leung LH, Fung AS, Daniel YT, Fong DQ, Dora LW, et al. White matter anisotropy in post-treatment childhood cancer survivors: preliminary evidence of association with neurocognitive function. J Clin Oncol. 2006; 24:884–889. https://doi.org/10.1200/JCO.2005.02.4505 PMID: 16484697

10. Froklage FE, Oosterbaan LJ, Sizoo EM, Groot M, Bosma I, Sanchez E, et al. Central neurotoxicity of standard treatment in patients with newly-diagnosed high-grade glioma: a prospective longitudinal study. J Neurooncol. 2014; 116:387–394. https://doi.org/10.1007/s11060-013-1310-4 PMID: 24264531

11. Schag CC, Heinrich RL, Ganz PA. Karnofsky performance status revisited: reliability, validity, and guidelines. J Clin Oncol. 1984; 2:187–193. https://doi.org/10.1200/JCO.1984.2.3.187 PMID: 6699671

12. Korlimarla A, Spiridigliozzi GA, Crisp K, et al. Novel approaches to quantify CNS involvement in children with Pompe disease. Neurology. 2020; 95(6):e718–e732. https://doi.org/10.1212/WNL.0000000000009979 PMID: 32518148

13. Forbes K. MRI brain white matter change: spectrum of change—how we can grade?. J R Coll Physicians Edinb. 2017; 47(3):271–275. https://doi.org/10.4997/JRCPE.2017.313 PMID: 29465106

14. Armstrong GT, Liu Q, Yasui Y, Huang S, Ness KK, Leisenring W, et al. Long-term outcomes among adult survivors of childhood central nervous system malignancies in the Childhood Cancer Survivor Study. J Natl Cancer Inst. 2009; 101:946–958. https://doi.org/10.1093/jnci/djp148 PMID: 19535780

15. Musial-Bright L, Fengler R, Henze G, Driever PH. Carboplatin and ototoxicity: hearing loss rates among survivors of childhood medulloblastoma. Childs Nerv Syst. 2011; 27:407–413. https://doi.org/10.1007/s00381-010-1300-1 PMID: 20931205

16. Orgel E, Jain S, Ji L, Pollick L, Si S, Finlay J, et al. Hearing loss among survivors of childhood brain tumors treated with an irradiation-sparing approach. Pediatr Blood Cancer. 2002; 58:953–958. Doi: 10.1002/pbc.23275

17. Duffner PK. Risk factors for cognitive decline in children treated for brain tumors. Eur J Paediatr Neurol. 2010; 14:106–115. https://doi.org/10.1016/j.ejpn.2009.10.005 PMID: 19931477

PLOS ONE

Age at diagnosis, posterior fossa tumors treatment and academic achievements

18. Tabori U, Sung L, Hukin J, Laperriere N, Crooks B, Carret AS, et al. Medulloblastoma in the second decade of life: a specific group with respect to toxicity and management: a canadian pediatric brain tumor consortium study. Cancer. 2005; 103:1874–1880. https://doi.org/10.1002/cncr.21003 PMID: 15770645

19. Monje M, Fisher PG.Neurological complications following treatment of children with brain tumors. J Pediatr Rehabil Med. 2011; 4:31–36. https://doi.org/10.3233/PRM-2011-0150 PMID: 21757808

20. Vargo M. Brain tumor rehabilitation. Am J Phys Med Rehabil. 2011; 90: S50–S62. https://doi.org/10.1097/PHM.0b013e31820be31f PMID: 21765264

21. Leung LH, Ooi GC, Kwong DL, Chan GC, Cao G, Kwong PL. White-matter diffusion anisotropy after chemo-irradiation: a statistical parametric mapping study and histogram analysis. Neuroimage. 2004; 21:261–268. https://doi.org/10.1016/j.neuroimage.2003.09.020 PMID: 14741664

22. Lassaletta A, Bouffet E, Mabbott D, Kulkarni AV. Functional and neuropsychological late outcomes in posterior fossa tumors in children. Childs Nerv Syst. 2015; 31: 1877–1890. https://doi.org/10.1007/s00381-015-2829-9 PMID: 26351237

23. Boman KK, Hovén E, Anclair M, Lannering B, Gustafsson G. Health and persistent functional late effects in adult survivors of childhood CNS tumours: a population-based cohort study. Eur J Cancer. 2009; 45:2552–2561. https://doi.org/10.1016/j.ejca.2009.06.008 PMID: 19616428

24. Zou P, Mulhern RK, Butler RW, Li CS, Langston JW, Ogg RJ. BOLD responses to visual stimulation in survivors of childhood cancer. Neuroimage. 2005; 24: 61–69. https://doi.org/10.1016/j.neuroimage.2004.08.030 PMID: 15588597

25. Khong PL, Leung LH, Chan GC, Kwong DL, Wong WH, Cao G, et al. White matter anisotropy in childhood medulloblastoma survivors: association with neurotoxicity risk factors. Radiology. 2005; 236: 647–652. https://doi.org/10.1148/radiol.2362041066 PMID: 16040920

26. Shan ZY, Liu JZ, Glass JO, Gajjar A, Li CHS, Reddick WE. Quantitative morphologic evaluation of white matter in survivors of childhood medulloblastoma. Magn Reson Imaging. 2006; 24:1015–1022. https://doi.org/10.1016/j.mri.2006.04.015 PMID: 16997071

27. Rueckriegel SM, Driever PH, Blankenburg F, Lüdemann L, Henze G, Bruhn H. Differences in supratentorial damage of white matter in pediatric survivors of posterior fossa tumors with and without adjuvant treatment as detected by magnetic resonance diffusion tensor imaging. Int J Radiat Oncol Biol Phys. 2010; 76:859–866. https://doi.org/10.1016/j.ijrobp.2009.02.054 PMID: 19540067

28. Winick N. Neurocognitive outcome in survivors of pediatric cancer. Curr Opin Pediatr. 2011; 23: 27–33. https://doi.org/10.1097/MOP.0b013e32834255e9 PMID: 21157347

PLOS ONE | https://doi.org/10.1371/journal.pone.0243998   December 16, 2020

12 / 12